AMERICAN SOCIETY FOR MICROBIOLOGY | Infection and Immunity

Pathogenesis and Host Response | Full-Length Text

# *Brucella* targets the host ubiquitin-specific protease, *Usp8*, through the effector protein, TcpB, for facilitating infection of macrophages

**Kiranmai Joshi,[1,2] Varadendra Mazumdar,[1,2] Binita Roy Nandi,[1,2] Girish K. Radhakrishnan[1]**

**AUTHOR AFFILIATIONS** See affiliation list on p. 21.

**ABSTRACT** *Brucella* species are Gram-negative intracellular bacterial pathogens that cause the worldwide zoonotic disease brucellosis. *Brucella* can infect many mammals, including humans and domestic and wild animals. *Brucella* manipulates various host cellular processes to invade and multiply in professional and non-professional phagocytic cells. However, the host targets and their modulation by *Brucella* to facilitate the infection process remain obscure. Here, we report that the host ubiquitin-specific protease, USP8, negatively regulates the invasion of *Brucella* into macrophages through the plasma membrane receptor, CXCR4. Upon silencing or chemical inhibition of USP8, the membrane localization of the CXCR4 receptor was enriched, which augmented the invasion of *Brucella* into macrophages. Activation of USP8 through chemical inhibition of 14-3-3 protein affected the invasion of *Brucella* into macrophages. *Brucella* suppressed the expression of *Usp8* at its early stage of infection in the infected macrophages. Furthermore, we found that only live *Brucella* could negatively regulate the expression of *Usp8*, suggesting the role of secreted effector protein of *Brucella* in modulating the gene expression. Subsequent studies revealed that the *Brucella* effector protein, TIR-domain containing protein from *Brucella*, TcpB, plays a significant role in downregulating the expression of *Usp8* by targeting the cyclic-AMP response element-binding protein pathway. Treatment of mice with USP8 inhibitor resulted in enhanced survival of *B. melitensis,* whereas mice treated with CXCR4 or 14-3-3 antagonists showed a diminished bacterial load. Our experimental data demonstrate a novel role of *Usp8* in the host defense against microbial intrusion. The present study provides insights into the microbial subversion of host defenses, and this information may ultimately help to develop novel therapeutic interventions for infectious diseases.

**KEYWORDS** *Brucella*, ubiquitin-specific protease (USP8), CXCR4, TIRAP, macrophages, CREB, host cell invasion, protein degradation, effector protein

Genus *Brucella* contains Gram-negative facultative intracellular bacterial pathogens, causing the worldwide zoonotic disease, brucellosis. *Brucella* can infect many mammals, including domestic and wild animals, marine mammals, and humans (1). Based on the differences in pathogenicity and host preferences, 12 species of *Brucella* are currently recognized such as *B. melitensis* (goat and sheep), *B. abortus* (cattle), *B. suis* (swine), *B. neotomae* (desert rat), *B. ovis* (sheep), and *B. canis* (dogs), *B. pinnipedialis* (seals), *B. ceti* (cetaceans), *B. microti (wood rat), B. papionis (baboons)*, and *B. inopinata* (humans) (*2*). Brucellosis is highly contagious, and the primary cause of human infection is consuming contaminated dairy products, inhaling *Brucella*-containing aerosols, or contact with infected materials. Acute human infection manifests as generalized symptoms, including fever, chills, headache, and fatigue. The chronic infection may lead to endocarditis and meningitis, which can be fatal (3). In animals, *Brucella* spp. cause

**Editor** Sunny Shin, University of Pennsylvania Perelman School of Medicine, Philadelphia, Pennsylvania, USA

Address correspondence to Girish K. Radhakrishnan, girish@niab.org.in.

The authors declare no conflict of interest.

See the funding table on p. 22.

**Received** 26 July 2023
**Accepted** 12 November 2023
**Published** 4 January 2024

abortions in the late trimester, stillbirths, retention of the placenta, and decreased milk production in females and infertility in males, which are the major consequences leading to substantial economic loss in the livestock industry worldwide (4, 5). Treatment of human *Brucellosis* involves prolonged oral regimens of doxycycline and streptomycin for 6 weeks, where 16% of individuals who undergo antibiotic treatment may show relapse (6). Frequent therapeutic failures also make antibiotic therapy for brucellosis ineffective. There is no human vaccine for brucellosis; the only option to control human infection is mass vaccination of susceptible animals. However, the available animal vaccines have significant drawbacks, including their infectivity to humans (7). Therefore, understanding the *Brucella*-host interaction is crucial to identify novel targets for developing improved vaccines and therapeutics for brucellosis.

*Brucella* spp. invade and multiply in macrophages, dendritic cells, trophoblasts, and epithelial cells (8). *Brucella* employs a secretion system to introduce bacterial effectors into the infected cells. These proteins interfere with host cellular pathways allowing the pathogen to resist intracellular killing and build an intracellular niche favorable for replication. *Brucella* harbors a type IV secretory system encoded by the VirB operon that is involved in the secretion of many effector proteins in the infected macrophages. These effector proteins interact with components of cellular pathways to generate replication-permissive, ER-derived compartments, leading to the chronic persistence of bacteria in the host (9). Since the interplay between bacterial effectors and the host cellular machinery plays a critical role in the invasion and persistence of *Brucella*, understanding these mechanisms is crucial for developing effective therapeutic and preventive measures for brucellosis. Studies have identified a few host proteins targeted by *Brucella* during their multistage intracellular cycle involving entry, trafficking, replication, and egress out of the host cells (10). Brucellae interact with GTPases belonging to the Rho subfamily, viz., Rho, Rac and CDC42 induces cytoskeleton remodeling during cell invasion (11). Many cell surface receptors such as CXCR4, CD36, and PrpC are reported to be induced by *Brucella* infection, which promotes entry into the macrophages (12, 13). Small GTPases such as Sar1 and Rab2 were reported to play an essential role in the intracellular replication of *Brucella* (14, 15). Brucellae are known to activate unfolded protein response (UPR) by phosphorylating IRE1 through Yip1 to form a replicative niche in the endoplasmic reticulum (16–18). They also target various components of host immune signaling pathways, including Toll-like receptors, to evade or suppress immune responses that contribute to their chronic persistence in the host (19–21). However, evidence suggests that *Brucella* manipulates host cellular processes and signaling pathways for their survival; our understanding of the *Brucella*-host interaction is still rudimentary compared to other invasive bacterial pathogens.

By employing an siRNA-based screening, we identified that the host ubiquitin-specific protease-8 (USP8) plays a crucial role in *Brucella* infection of macrophages. USP8 is a promiscuous deubiquitinating enzyme that counterbalances the ubiquitination harnessed by numerous E3 ligases (22). It is a multidomain protein containing a microtubule-interacting domain, transport domain (MIT), SH3-binding motifs (SH3-BM), 14-3-3-peptide-binding motif, and the catalytic domain with deubiquitinase property. USP8 has pleiotropic functions inside the cells and maintains cellular homeostasis by regulating protein turnover and cargo sorting. It maintains the dynamic state of cellular ubiquitome by removing the conjugated ubiquitin moiety from the substrate proteins. USP8 selectively interacts with a palette of substrates through its substrate-binding motif and is involved in sorting out various membrane receptors for either recycling or degradation (23). USP8 is reported to regulate endosomal trafficking by stabilizing the endosomal sorting complex (ESCRT-0) through deubiquitinating the scaffold proteins Hrs and STAM1/2 (24). We observed that the silencing of USP8 enhanced the uptake of *Brucella* into macrophages, whereas its overexpression suppressed the *Brucella* invasion. In addition, USP8 affected the interaction of *Brucella* with macrophages through the regulation of the availability of the plasma membrane receptor, CXCR4. Furthermore, we found that *Brucella* suppressed the expression of USP8 at the initial stages of its infection

through the effector protein, TcpB. The modulation of USP8 activity using the inhibitors or activators affected the splenic load of *B. melitensis* in the infected mice. Our research findings uncovered a novel role of the host protein, USP8, which plays a vital role in the defense against infectious diseases. The study also signified the strategies employed by the infectious pathogens to counteract this host defense mechanism to establish the infection.

## MATERIALS AND METHODS

### Cell culture

Immortalized bone marrow-derived macrophages from mice (iBMDMs; a gift from Petr Broz, University of Lausanne) and human embryonic kidney (HEK) 293T cells (ATCC# CRL-3216) were cultured in Dulbecco's Modified Eagle's Medium (DMEM; Sigma) supplemented with 10% fetal bovine serum (Sigma) and 1× penicillin-streptomycin solution (Gibco). Roswell Park Memorial Institute (RPMI 1640; Sigma) supplemented with 10% fetal bovine serum and 1× penicillin-streptomycin solution was used to culture the murine macrophage cell line, J774 (ATCC# TIB-67). The cells were grown in a humidified atmosphere of 5% $CO_2$ at 37°C. The iBMDMs were differentiated using macrophage colony-stimulating factor (BioLegend; 20 ng/mL).

### Culturing of *Brucella*

*B. neotomae* was grown in brucella broth or brucella agar (BD). *ΔTcpB B. neotomae* was cultured in brucella broth or agar with kanamycin (40 µg/mL). Same media with kanamycin (40 µg/mL) and chloramphenicol (50 µg/mL) were used for culturing *ΔTcpB::TcpB B. neotomae*. For infection studies, *B. neotomae* strains were pelleted down at 1.0 OD and washed thrice with 1× PBS (Phosphate buffered saline). The pellet was then resuspended in 1 mL of 1× PBS (pH 7.4) and used for infecting the macrophages at an MOI (Multiplicity of Infection) of 1,000:1. *B. melitensis* was cultured similar to wild-type *B. neotomae* and infected with an MOI of 200:1. To examine the mRNA expression levels of *TcpB* in different growth phases, single colony of *B. neotomae* was inoculated into the brucella broth and grown at 37°C with shaking in the presence of 5% $CO_2$. The bacteria were then harvested at lag (0.2 OD), log (0.6 OD), and stationary (1.0 OD) phases, and the total RNA was isolated using the RNA Extraction Kit (MN) as per manufacturer's instructions.

### Silencing and overexpression of *Usp8* in macrophages

To silence the *Usp8* gene in iBMDMs, a set of four siRNAs was procured from Dharmacon (ON-TARGET plus SMART pool). The iBMDMs were seeded ($5 \times 10^4$ cells/well) into 24-well plates and transfected with 50 picomoles of siUsp8 or non-target (NT) siRNA in duplicates using Dharmafect 4.0 transfection reagent as per manufacturer's protocol. To examine the silencing of USP8 in iBMDMs, the cells were harvested 48 hours post-transfection, followed by total RNA isolation and cDNA synthesis. Subsequently, qRT-PCR analysis was performed using *Usp8*-specific primers to quantify the mRNA expression levels of *Usp8*. Data were normalized with the endogenous control, *Gapdh*. Furthermore, the siRNA-transfected iBMDMs were subjected to immunoblotting using the anti-USP8 antibody to detect the endogenous levels of USP8. Actin was used as the loading control.

To overexpress *Usp8*, iBMDMs were seeded ($5 \times 10^4$ cells/well) into 24-well plates and allowed to adhere overnight. Next, the cells were transfected with the eukaryotic expression plasmid harboring *Usp8* (pCMV-HA-*Usp8*) or empty vector (pCMV-HA) using X-fect (TAKARA Bio) transfection reagent, according to the manufacturer's instructions. The overexpression of *Usp8* in iBMDMs was confirmed by qRT-PCR and immunoblotting, as described below.Plasmids used for transfection are listed in Table 3.

### Silencing of *Cxcr4* in macrophages

To silence endogenous *Cxcr4* gene in iBMDMs, the *Cxcr4*-specific short hairpin RNA (shRNA) (25) and the non-target control shRNA (26) were used. The sense and anti-sense shRNA oligonucleotides were synthesized, followed by annealing the oligos and cloning into the shRNA expression plasmid, pLKO-1 (gift from Dr. D. Root, plasmid #10878; Addgene). The iBMDMs were transfected with *Cxcr4*-specific or control shRNA construct. Forty-eight hours post-transfection, the silencing of endogenous *Cxcr4* was assessed by qRT-PCR and immunoblotting using anti-CXCR4 antibody. The sequences of sense strands of shRNA oligonucleotides are given below:

*Cxcr4*-specific shRNA: 5′CCGGTACCTCGCCATTGTCCACCTGCAG GTGGACAATGGCGAGG TATTTTTG3′

Non-target shRNA: 5′CCGGTTCTCCGAACGTGTCACGTTTCTGCAGAAACGTGACACGTTC GGAGAATTTTTG3′

### Infection of macrophages with *B. neotomae* or *B. melitensis*

To perform infection studies using *Usp8*-silenced iBMDMs, the cells were first transfected with siRNA. Forty-eight hours post-transfection, the cells were infected with *B. neotomae* (ATCC 23459–5K33) at an MOI of 1,000:1 or *B. melitensis* 16M (obtained from Indian Veterinary Research Institute) at an MOI of 200:1. After the addition of *Brucella*, the plates were centrifuged at 280 × *g* for 3 min to pellet down the bacteria onto the cells. Subsequently, the plates were incubated for 90 min at 37°C with 5% $CO_2$. Next, the cells were washed three times with 1× PBS (pH 7.4) and treated with gentamicin (30 µg/mL) for 30 min to kill extracellular *Brucella*. The infected cells were maintained in the cell culture media containing 3 µg/mL of gentamicin. Next, the cells were lysed with 0.1% Triton X-100 in PBS at various hours post-infection, followed by serial dilution of lysates and plating on *Brucella* agar (BD). The intracellular load of *Brucella* was quantified by enumerating the CFU, and the data were represented as CFU/mL. To perform infection studies using USP8-overexpressing iBMDMs, the cells were infected with *B. neotomae* or *B. melitensis* 16M 24 hours post-transfection as described before.

For the invasion assay, *B. neotomae* or *B. melitensis* was added to the multi-well plates harboring the macrophages, followed by centrifuging the bacteria onto the cells. Subsequently, the plates were incubated for 30 min at 37°C with 5% $CO_2$. Next, the cells were washed thrice with PBS and treated with 30 µg/mL gentamicin for 30 min to kill extracellular *Brucella*. Subsequently, the infected cells were lysed with 0.1% Triton X-100 in PBS, then serial dilution of lysates and plating on *Brucella* agar. Finally, the intracellular *Brucella* was quantified by enumerating the CFU. To perform invasion assay using USP8-overexpressing iBMDMs, the cells were transfected with pCMV-HA-*Usp8* or empty vector (pCMV-HA) as described previously. Twenty-four hours post transfection, the cells were infected with *B. neotomae* for invasion assay as described above.

To perform macrophage invasion assay with *B. neotomae* or *B. melitensis* in the presence of inhibitors of USP8 (DUB-IN-2; MedChem; 10 µM) or CXCR4 (AMD3100; Sigma, 10 µM) or cyclic-AMP response element-binding protein (CREB; CREB Inhibitor; Sigma, 5 µM), iBMDMs were treated with CREB inhibitor for 3 hours or USP8 and CXCR4 inhibitor for 24 hours, followed by infection with *B. neotomae* or *B. melitensis* for 30 min and CFU analysis. For analyzing the *Brucella* invasion in the presence of the USP8 activator (BV02, Sigma, 20 µM), iBMDMs were treated with BV02 for 24 hours, followed by *Brucella* invasion assay as described before. The vehicles, such as DMSO (for USP8, CREB inhibitor, and USP8 activator) and PBS (for CXCR4), were used as the controls.

To perform macrophage invasion assay with *B. neotomae* or *B. melitensis* in *Cxcr4*-silenced macrophages, iBMDMs were transfected with *Cxcr4* shRNA or non-target control shRNA construct. Forty-eight hours post-transfection, cells were infected with *B. neotomae* or *B. melitensis*, followed by invasion assay as described before.

To evaluate the endogenous protein levels of USP8 or CREB/p-CREB, iBMDMs were infected with either *B. neotomae* or *B. melitensis*. The cells were harvested at various time points post-infection, followed by cell lysis in RIPA buffer. The lysates were then clarified,

and the amount of total protein in the samples was quantified using the Bradford assay (Sigma). Subsequently, the samples were subjected to immunoblotting, and the levels of USP8 or CREB/p-CREB were detected using the respective primary antibodies and horseradish peroxidase (HRP)-conjugated secondary antibodies (Table 1).

To examine the expression of *Usp8* in the macrophages infected with heat-killed *Brucella*, *B. neotomae* was heat inactivated by incubating the culture at 60°C for 1 hour in a water bath. Subsequently, the inactivation of *B. neotomae* was confirmed by streaking the culture on *Brucella* agar plates. Next, iBMDMs were infected with heat-killed *B. neotomae*, and then the target gene expression was analyzed by qRT-PCR and immunoblotting.

## Immunoblotting

The harvested cells were lysed in radioimmunoprecipitation assay buffer (10 mM Tris HCL pH 8.0, 1 mM EDTA, 1% TritonX-100, 0.1% SDS, 40 mM NaCl) buffer with a protease inhibitor cocktail (Pierce). The amount of total protein in the samples was quantified using the Bradford assay (Sigma). An equal concentration of protein samples was mixed with 2× Laemmli buffer (BioRad), and the samples were boiled for 10 min at 100°C. Next, the protein samples were resolved on SDS-PAGE gel, followed by the transfer of protein onto the PVDF membrane (Merck Millipore) using a wet-tank blotting system (Bio-Rad). The membrane was blocked with 5% skimmed milk in Tris-buffered saline with Tween 20 (TBST; Cell Signaling Technology) for 1 hour, followed by incubation with the respective primary antibody overnight at 4°C. Next, the membrane was washed three times with TBST and incubated with horseradish peroxidase-conjugated secondary antibody. Next, the primary or secondary antibody was diluted in 5% skimmed milk in TBST. Finally, the membrane was washed three times with TBST and incubated with Super Signal West Pico or Femto chemiluminescent substrate (Pierce). The signals were captured using a chemi-documentation system (Syngene). The antibody source and dilutions used are listed in Table 1.

## Gene expression analysis using quantitative RT-PCR

To analyze the expression of *Usp8* in the *Brucella*-infected cells by qRT-PCR, iBMDMs were seeded into 24-well plates ($5 \times 10^4$ cells/well) in DMEM supplemented with 10% FBS without antibiotics and incubated overnight at 37°C with 5% $CO_2$. The cells were infected with *B. neotomae* (live or heat killed) at an MOI of 1,000:1 or *B. melitensis* at an MOI of 200:1 as described before, followed by harvesting the cells at various time points. The total RNA was isolated from the infected macrophages using RNAiso PLUS (Takara Bio), followed by the preparation of cDNA using PrimeScript RT Reagent Kit (Takara Bio) as per the manufacturer's protocol. The qRT-PCR was performed using gene-specific primers

**TABLE 1** Details of antibodies used for the study

| S. no | Antibody | Manufacturer | Dilution |
|---|---|---|---|
| 1. | Anti-FLAG HRP conjugated | Sigma | 1:5,000 |
| 2. | Anti-HA HRP conjugated | Sigma | 1:5,000 |
| 3. | Anti-actin HRP conjugated | Sigma | 1:25,000 |
| 4. | Anti-USP8 | Thermo Fisher Scientific | 1: 1,000 |
| 5. | Anti-CXCR4 | Invitrogen | 1: 1,000 (WB),1:500 (IF) |
| 6. | Anti-p-CREB | Cell Signaling Technology | 1: 1,000 |
| 7. | Anti-CREB | Cell Signaling Technology | 1: 1,000 |
| 8. | Anti-rabbit HRP conjugated | Cell Signaling Technology | 1:5,000 |
| 9. | Anti-mouse HRP conjugated | Cell Signaling Technology | 1:5,000 |
| 10. | Anti-calreticulin | Invitrogen | 1:200 |
| 11. | Anti-rabbit IgG Alexa Fluor 647 | Cell Signaling Technology | 1:500 |
| 12. | Anti-HA-FITC antibody | Sigma | 1:500 |
| 13. | Anti-TNFR1 | R&D | 1:500 |

**TABLE 2** Primer sequences of genes used for qRT-PCR analysis

| S. no | Gene | Sequence |
|---|---|---|
| 1. | Gapdh forward | 5′-AACGACCCCTTCATTGAC-3′ |
| 2. | Gapdh reverse | 5′-CCACGACATACTCAGCAC-3′ |
| 3. | Usp8 forward | 5′-AGACTCTCCGAAAGCCTTAAACT-3′ |
| 4. | Usp8 reverse | 5′-GCCGTTAATCCTTTGGGTTTTGG-3′ |
| 5. | Tirap forward | 5′-CTCCTACTTGGAAGGCAGCAC-3′ |
| 6. | Tirap reverse | 5′-ACGAAAGCCACCATCAGGG-3′ |
| 7. | Myd88 forward | 5′-TGCTGGAGCTGGGACCCAGCATTGAGGA-3′ |
| 8. | Myd88 reverse | 5′-TCAGACACACACACAACTTCAGTCGATA-3′ |

with the SYBR Green method using the real-time PCR machine (BioRad). The relative gene expression was analyzed by the comparative $2^{-\Delta\Delta Ct}$ method using CFX96 software (BioRad). Data were normalized with the endogenous control, *Gapdh*. To examine the downregulation of target gene expression by siRNA, the cells were harvested 48 hours post-transfection, followed by RNA isolation, cDNA preparation, and qRT-PCR analysis. The overexpression of USP8 in macrophages was also confirmed by qRT-PCR analysis, as described before. All the primers used for analyzing the gene expression by qRT-PCR are listed in Table 2.

To assess the levels of USP8 in the macrophages overexpressing TcpB, iBMDMs were seeded into 24-well plates ($5 \times 10^4$ cells/well) and transfected with 600 ng and 1,200 ng of the eukaryotic expression vector (pCMV-HA; Clontech) harboring *TcpB* (pCMV-HA-*TcpB*) for 24 hours. Subsequently, the cells were collected and processed for qRT-PCR and immunoblotting as described before.

To analyze the expression of *TcpB* in *B. neotomae*, the bacterial cultures were harvested at lag, log, or stationary phase, followed by the extraction of total RNA, preparation of cDNA, and qRT-PCR analysis. The data were normalized with the endogenous control, 16S rRNA of *Brucella*.

## Preparation of membrane fraction

The total membrane fraction containing the CXCR4 protein was isolated from iBMDMs, as mentioned elsewhere (27). Briefly, iBMDMs were sonicated in 100 µL buffer containing 100 mM Tris-HCl pH 10.7, 5 mM EDTA, and 2 mM DTT at 4°C. After sonication, the sample was diluted to 500 µL with buffer containing 100 mM Tris-HCl pH 8, 0.33 M sucrose, 5 mM EDTA, and 2 mM DTT. Next, the sample was centrifuged for 3 min at 1,000 *g* at 4°C. Then, the supernatant was collected and centrifuged again for 5 min at 3,000 *g* at 4°C. Finally, the resulting supernatant was centrifuged at 19,000 *g* for 45 min at 4°C, followed by the collection of pellets corresponding to the total membrane fraction. The pellet was then dissolved in 50 µL buffer containing 10 mM Tris-HCl pH 7.5, 0.1 mM DTT, and 20% glycerol for further experiments.

## Immunofluorescence microscopy

To generate *B. neotomae*-expressing Green Fluorescent Protein (GFP), the *Brucella* expression plasmid harboring GFP (pNSTrcd-GFP) was electroporated into *B. neotomae* using a Micro Pulser (Bio-Rad). The transformants were selected on *Brucella* agar containing chloramphenicol (40 µg/mL). To perform confocal microscopy analysis, macrophages infected with *B. neotomae*-GFP were washed with PBS and fixed with 4% paraformaldehyde for 20 min at room temperature (RT). The cells were then permeabilized with 0.1% Triton X-100 in PBS for 10 min. Subsequently, the cells were blocked with 1% Bovine Serum Albumin (BSA) in PBS containing 50 mM $NH_4Cl$ for 30 min at RT. The cells were then incubated with the anti-calreticulin antibody for 1 hour at RT, followed by Alexa Fluor 647-conjugated secondary antibody for 1 hour at RT to stain the endoplasmic reticulum. Finally, the cells were mounted in Prolong Gold antifading agent with DAPI (Thermo Fisher Scientific). The cells were analyzed using a laser confocal

microscope at 40× magnification (Leica). To perform fluorescence microscopy, the *B. neotomae*-GFP-infected cells were fixed with 4% paraformaldehyde in PBS, followed by staining of the nucleus with Hoechst stain (Thermo Fisher Scientific). The images were captured using a fluorescent microscope (Carl Zeiss) at 20× magnification. Fifteen fields were analyzed from the samples transfected with NT and siUSP8 and quantified using Image J software.

To perform immunofluorescence microscopy for analyzing membrane localization of CXCR4 in USP8-overexpressing cells, HEK 293T cells were seeded onto glass bottom dishes ($0.5 \times 10^6$ cells/dish) in DMEM supplemented with 10% FBS and allowed to adhere overnight at 37°C with 5% $CO_2$. Cells were then transfected with eukaryotic expression plasmid harboring USP8 (pCMV-HA-*Usp8*) or empty vector using the X-fect transfection reagent. Twenty-four hours post-transfection, cells were washed with PBS and fixed with 4% paraformaldehyde for 20 min at RT, followed by permeabilization with 0.1% Triton X 100 in PBS. Cells were then blocked with 1% BSA in PBS containing 50 mM $NH_4Cl$. Next, the cells were stained with the anti-CXCR4 antibody, followed by AlexaFluor-647 secondary antibody, and HA-USP8 was stained with mouse anti-HA-FITC antibody (Table 1) at RT. Finally, the cells were mounted in Prolong Gold anti-fading agent with DAPI. The cells were analyzed using a fluorescence microscope (Carl Zeiss) at 20× magnification. To analyze the membrane localization of CXCR4 with USP8 inhibitor, iBMDMs were treated with DMSO or DUB-IN-2 (10 µM) for 24 hours. Subsequently, the cells were stained for CXCR4 as described above and analyzed using a laser confocal microscope (Leica) at 63× magnification. To analyze the membrane localization of CXCR4 with USP8 inhibitor, iBMDMs were treated with DMSO or DUB-IN-2 (10 µM) for 24 hours. Subsequently, the cells were processed for confocal microscopy as described above. Twelve different fields were analyzed from DUB-IN-2 or DMSO-treated samples.

To examine the invasion of *Brucella* in *Usp8*-overexpressing cells, iBMDMs were transfected with pCMV-HA-*Usp8*(HA-*Usp8*) or empty vector using the X-fect transfection reagent. Twenty-four-hour post-transfection, the cells were infected with *B. neotomae*-GFP, followed by processing the cells for fluorescent microscopy as described before. The cells were analyzed using a fluorescence microscope (Carl Zeiss) at 20×magnification, and *B. neotomae*-GFP per well was quantified using ImageJ software. Twelve different fields were analyzed for each sample.

## Cytotoxicity assay

To examine the cytotoxicity of DUB_IN-2 (USP8 inhibitor) and BV02 (14-3-3 inhibitor), iBMDMs were seeded into a 48-well plate and allowed to adhere overnight. The cells were treated with 5, 10, 15, and 20 µM of either DUB_IN-2/BV02 or DMSO for 24 hours. The supernatants were collected, then the released lactate dehydrogenase (LDH) level was quantified using CytoTox 96 (Promega) as per the manufacturer's protocol. The untreated cells lysed with 0.1% Triton X100 served as the high control for the LDH assay. The AMD3100 and CREB inhibitors (666-15) were not known to cause any toxicity to the normal cells (28, 29).

## Co-transfection and protein degradation experiments

To examine the role of *Brucella* effector proteins, TcpB, CbpB, and BspI, on the expression of *Usp8*, HEK293T cells were transfected with the eukaryotic expression plasmids, pCMV-HA-*TcpB*(HA-*TcpB*), pCMV-HA-*CbpB*(HA-*CbpB*), and pCMV-FLAG-*Bsp*I (FLAG-*Bsp*I). HEK293T cells were seeded into 12-well plates ($1 \times 10^5$ cells/well) and transfected with two concentrations (600 and 1,200 ng) of *TcpB, CbpB,* and *Bsp*I plasmids. Twenty-four hours post-transfection, the cells were harvested and processed for immunoblotting as described previously. The blots were probed with HRP-conjugated anti-HA and anti-FLAG to detect TcpB, CbpB, and BspI proteins, respectively, and the endogenous level of USP8 was detected using the anti-USP8 antibody, followed by HRP-conjugated anti-mouse IgG. To examine the mRNA expression of *Usp*8, *Tirap,* and *Myd88*, HEK293T cells were transfected with HA-*TcpB*. Twenty-four hours post-transfection, the cells were

harvested and processed for RNA isolation and cDNA synthesis. Subsequently, qRT-PCR was performed to quantify the expression levels of *Usp8, Tirap,* and *Myd88*.

To examine the endogenous levels of TIRAP, p-CREB, and USP8 in the presence of TcpB, HEK 293T cells were seeded in 12-well ($1 \times 10^5$ cells/well) plates and transfected with two concentrations (600, and 1,200 ng) of HA-*TcpB*. Twenty-four hours post-transfection, cells were harvested and processed for immunoblotting to examine the protein levels as described earlier. To determine whether the purified maltose-binding protein (MBP)-TcpB protein affects USP8 levels, iBMDMs were treated with purified MBP-TcpB protein or MBP alone (5 µg/mL) for 5 hours, followed by harvesting the cells and immunoblotting to detect the endogenous levels of USP8 protein. To analyze the degradation of TIRAP by TcpB, HEK293T cells were co-transfected with pCMV-FLAG-*Tirap* (FLAG-*Tirap*) (300 ng) with two concentrations of HA-*TcpB* (600, and 1,200 ng). Twenty-four hours post-transfection, cells were harvested and subjected to immunoblotting to detect the expression levels of FLAG-TIRAP and HA-TcpB.

To examine whether overexpression of *Tirap* leads to stabilization of USP8, HEK293T cells were transfected with FLAG-*Tirap* (1.2 µg). Twenty-four hours post-transfection, cells were harvested and processed for immunoblotting to assess the levels of p-CREB and USP8. For titrating the effect of TcpB on TIRAP-mediated expression of *Usp8*, HEK293T cells were transfected with HA-*TcpB* (600 ng) and two concentrations of FLAG-*Tirap* (600 and 1,200 ng) for 24 hours. Subsequently, the cells were harvested and subjected to immunoblotting to detect the endogenous levels of USP8. Primary antibodies used for detecting TIRAP and p-CREB are listed in Table 1. The HRP-conjugated anti-rabbit and anti-mouse secondary antibodies were used to detect TIRAP, p-CREB, and USP8, respectively. Plasmids used for co-transfection studies are listed in Table 3.

## Construction of *TcpB* knockout *B. neotomae*

A homologous recombination-based gene replacement technique was used for deleting the *TcpB* gene from *B. neotomae*. A three-way ligation was performed to generate the Δ*TcpB* plasmid. The 1 kb fragments, upstream and downstream of the *TcpB* gene, were amplified from the chromosomal DNA of *B. neotomae*. The forward and reverse primers for amplifying the upstream fragment harbored *Kpn*I and *Bam*HI restriction enzymes, respectively. The *Bam*HI and *Eco*RI sites were added in the forward and reverse primers, respectively, to amplify the downstream fragment. The kanamycin expression cassette from the pUC-kan-loxp plasmid was released with *Bam*HI digestion. The pZErO-1.1 plasmid (Invitrogen) was digested with *Kpn*I and *Xho1*, followed by ligating the upstream fragment with *Kpn*I and *Bam*HI, kanamycin cassette with *Bam*HI, and the downstream fragment with *Bam*HI and *Eco*RI restriction sites. The plasmid was transformed into DH5α, and the positive clones were confirmed by selecting on Zeocin (50 µg/mL) and kanamycin (50 µg/mL) plates. Subsequently, the Δ*TcpB* plasmid was introduced into *B. neotomae* by electroporation. The upstream and downstream fragments in the KO plasmid recombine with the respective sequences on the chromosomal DNA of *B. neotomae,* replacing the *TcpB* gene with the kanamycin expression cassette. The transformed *B. neotomae* colonies growing on kanamycin and Zeocin, which indicates a single recombination event and the resulting insertion of the KO plasmid into the

**TABLE 3** Plasmids used in the study

| S. no | Name of the plasmid | Origin of the plasmid | Selection markers |
|---|---|---|---|
| 1. | pUC-kan-loxp | Constructed in-house | Ampicillin |
| 2. | pZero 1.1 | Invitrogen | Kanamycin |
| 3. | pCMV-FLAG-Tirap | Addgene | Ampicillin |
| 4. | pCMV-HA-Usp8 | Addgene | Ampicillin |
| 5. | pCMV-HA-TcpB | Clontech | Ampicillin |
| 6. | pCMV-HA-CbpB | Clontech | Ampicillin |
| 7. | pCMV-FLAG-BspI | Clontech | Ampicillin |

chromosomal DNA, were discarded. The Zeocin-sensitive and kanamycin-resistant Δ*TcpB B. neotomae* colonies were selected and confirmed further by PCR.

To express *TcpB* in the Δ*TcpB B. neotomae* for complementation experiments, the *TcpB* gene was cloned into the *Brucella* expression plasmid, pNSTrcD, at the *Sal*I and *Xho*I sites. *B. neotomae* harboring pNSTrcD-*TcpB* was selected on *Brucella* agar plates with chloramphenicol (40 µg/mL). Plasmids used for construction of Δ*TcpB B. neotomae* and *TcpB* complemented *B. neotomae* are listed in Table 3.

### *In vivo* studies on mice using *B. melitensis*

To study the *in vivo* effect of chemical inhibition or activation of USP8 or inhibition of CXCR4 in the mice model of brucellosis, 8-week-old female BALB/c mice (four mice per group) were infected intraperitoneally with *B. melitensis* ($2.5 \times 10^6$ CFU per mouse) in 100 µL of 1× PBS. Ten days post-infection, mice were treated intraperitoneally with DUB_IN-2 (3 mg/kg) or BV02 (3 mg/kg), AMD3100 (1 mg/kg), or vehicle control for 3 days. Mice were euthanized by $CO_2$ asphyxiation on day 14, followed by the collection of spleens and CFU analysis to quantify the load of *B. melitensis* in the spleen. Furthermore, to correlate the *in vitro* data, 8-week-old female BALB/c mice (three mice per group) were pre-treated with CXCR4 inhibitor, AMD3100 (1 mg/kg), or vehicle control (PBS) for 24 hours. The next day, drug-treated mice were infected with *B. melitensis* as described above. Subsequently, the infected mice were treated with the drug on third, fifth, and seventh day, followed by euthanization and collection of spleen for CFU analysis to quantify the load of *B. melitensis*.

### Statistical analysis

GraphPad Prism 6.0 software was used for the statistical analysis of experimental data. Data are shown as the mean ± standard deviation (SD) or standard error of the mean (SEM). Statistical significance was determined by *t*-tests (two-tailed) for pairwise comparison. A one-way analysis of variance test was used to analyze the data involving more than two samples.

## RESULTS

### *Usp8* plays an essential role in the *Brucella*-macrophage interaction

We identified the role of *Usp8* in the *Brucella*-macrophage interaction while performing an siRNA screening using *B. neotomae*, which is reported to be the model pathogen to study brucellosis (30) (Fig. S1A). The expression of *Usp8* in iBMDMs was downregulated by treating the cells with *Usp8*-specific siRNA. The iBMDMs treated with si*Usp8* exhibited a diminished expression of *Usp8*, confirmed by qRT-PCR and immunoblotting (Fig. 1A and B). We observed an enhanced intracellular load of *B. neotomae* in iBMDMs treated with si*Usp8* compared to the cells transfected with non-targeting control siRNA (Fig. 1C). Therefore, we wished to perform detailed studies to understand the role of *Usp8* in the *Brucella*-macrophage interaction. To study the effect of *Usp8* on the intracellular survival of *Brucella*, iBMDMs were treated with si*Usp8* or NT, followed by infection with *B. neotomae* and analysis of CFU at various time points post-infection. The CFU analysis indicated that the intracellular load of *B. neotomae* was significantly enhanced in the *Usp8*-silenced macrophages at various time points post-infection (Fig. 1D). Since we observed a high bacterial load even at the early stages of infection, we performed an invasion assay to examine whether *Usp8* plays any role in the uptake of *Brucella* by macrophages. iBMDMs were treated with si*Usp8* or NT, followed by infection with *B. neotomae* or *B. neotomae*-GFP for 30 min and treated with gentamicin to kill the extracellular *Brucella*. The CFU analysis showed a remarkable enhancement of *B. neotomae* invasion in the *Usp8*-silenced cells compared to the control (Fig. 1E). Next, we infected *Usp8*-silenced macrophages with the zoonotic species of *Brucella*, *B. melitensis,* which also showed an enhanced invasion in the *Usp8*-downregulated iBMDMs (Fig. 1F). Similarly, the fluorescent microscopy analysis showed an enhanced

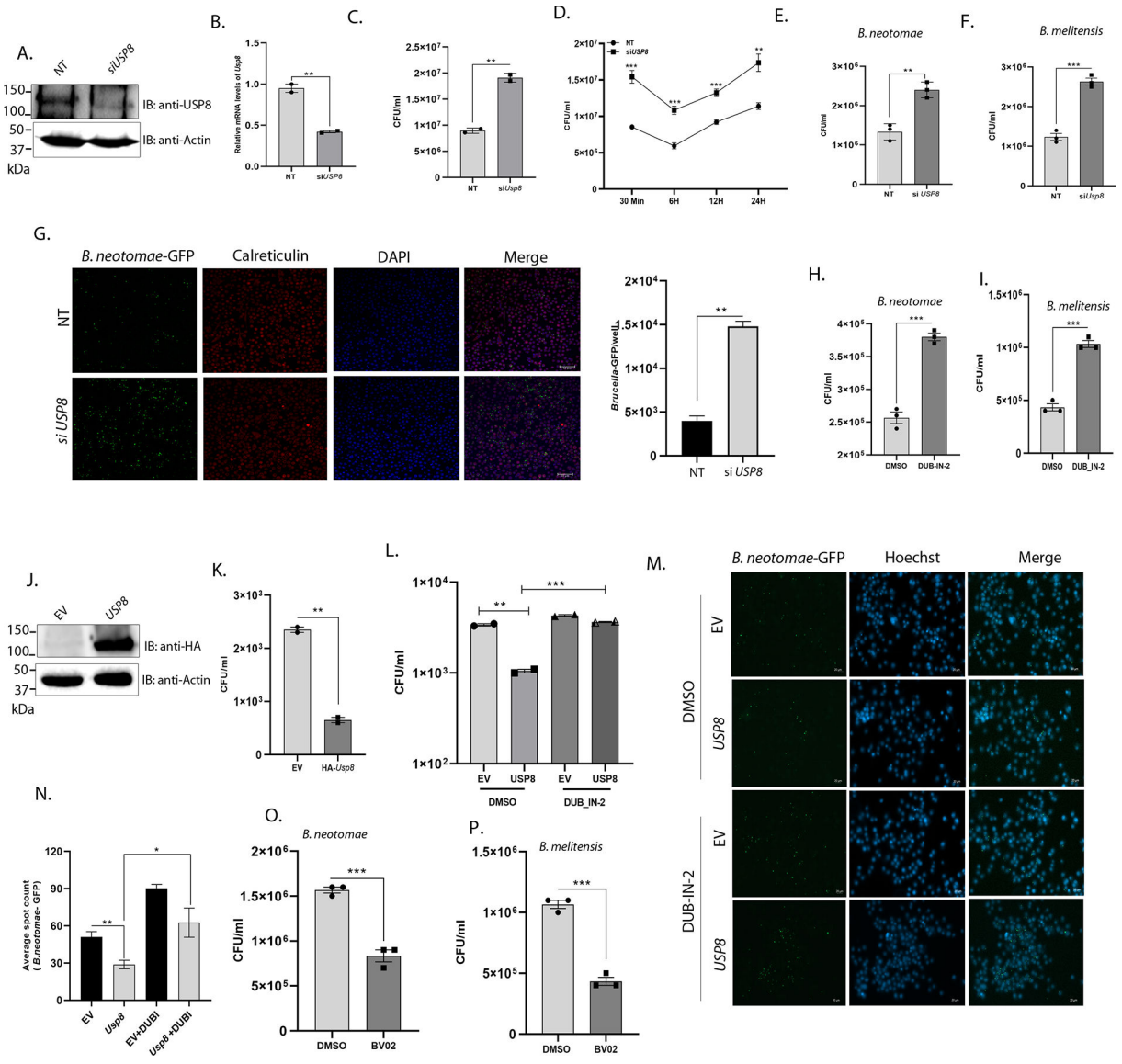


**FIG 1** USP8 plays an essential role in the invasion of *Brucella* into the macrophages. (Panels A and B) *Usp8* expression in cells treated with si*Usp8* or NT. The cells were treated with siRNAs for 48 hours, followed by analyzing the levels of *Usp8* by immunoblotting (A) and qRT-PCR (B). (Panels C and D) CFU analysis of *B. neotomae* isolated from *Usp8*-silenced or control iBMDMs. The cells were infected with *B. neotomae*, followed by isolation of bacteria at 24 hpi (C) or at indicated times (D) pi. (Panels E and F) *Brucella* invasion assay in *Usp8*-silenced or control iBMDMs. iBMDMs were treated with siUSP8 or NT, followed by infection with *B. neotomae* or *B. melitensis* for 30 min followed by gentamicin treatment for 30 min to kill extracellular bacteria and quantification of invaded *B. neotomae* by CFU count (E) or *B. melitensis* (F) by CFU enumeration. (G) *Brucella* invasion assay, followed by analyzing the invaded *B. neotomae*-GFP by confocal microscopy. The cells were stained with anti-calreticulin and Alexa Fluor 647-conjugated secondary antibody to visualize the endoplasmic reticulum (red). The nuclei were stained with DAPI (blue), which was present in the mounting reagent. Scale bar, 20 µm. The right panel indicates the quantification of intracellular *B. neotomae*-GFP using Harmony high-content analysis software. (Panels H and I) *Brucella* invasion assay in the presence of USP8 inhibitor. iBMDMs were treated with DUB_IN-2 or DMSO (vehicle) for 24 hours, followed by infection with *B. neotomae* (H) or *B. melitensis* (I) and CFU analysis. (J) Immunoblot showing the overexpression of USP8 in iBMDMs. Cells were transfected with HA-*Usp8* or EV. Twenty-four hours post-transfection, the cells were lysed, and the lysates were subjected to immunoblotting. The membrane was probed with HRP-conjugated anti-HA antibody to detect the overexpressed HA-USP8. (K) *Brucella* invasion assay using iBMDMs overexpressing HA-USP8. iBMDMs were transfected with HA-*Usp8*, followed by infection with *B. neotomae* and quantification of invaded bacteria by CFU enumeration. (Panels L and M) *Brucella* invasion assay using iBMDMs overexpressing HA-*Usp8* in the presence or absence of USP8 inhibitor. iBMDMs overexpressing *Usp8* were treated with DUB_IN-2 or DMSO, followed by infection with *B. neotomae* or *B. neotomae*-GFP. The invasion of *B. neotomae* and *B. neotomae*-GFP was examined by CFU enumeration (L) and fluorescence microscopy (M), respectively. (N) Average spot count of *B. neotomae*-GFP of each panel using ImageJ software. (Panels O and P) *Brucella* invasion assay using iBMDMs treated with 14-3-3ζ inhibitor, BV02. The cells were treated with BV02 or DMSO for 24 hours, followed by infection with *B. neotomae* (O) or *B. melitensis* (P) and CFU analysis. A representative result from at least two biological replicates is shown. The data are presented as means ± SD (*$P < 0.05$; **$P < 0.01$; ***$P < 0.001$). CFU, colony-forming unit; EV, empty vector; GFP, green fluorescence protein.

number of *B. neotomae*-GFP in the si*Usp8*-treated iBMDMs compared to the control (Fig. 1G). Furthermore, to validate the role of *Usp8* on the invasion of *Brucella*, we inhibited USP8 using the compound, DUB-IN-2, followed by infection studies using *B. neotomae* or *B. melitensis*. DUB-IN-2 was reported to inhibit the USP8, and treatment of iBMDMs with DUB-IN-2 for 24 hours neither induced any cytotoxicity nor modulated the expression of USP8 (31) (Fig. S1B and C). Next, the inhibitor or the vehicle (DMSO)-treated iBMDMs were infected with *B. neotomae* or *B. melitensis*, followed by the CFU analysis. In agreement with the silencing data, chemical inhibition of USP8 also showed an enhanced invasion of both *B. neotomae* and *B. melitensis* into macrophages (Fig. 1H and I).

To further confirm the experimental data, we overexpressed *Usp8* in the murine macrophages and then analyzed the invasion of *B. neotomae*. To overexpress Usp8, the iBMDMs were transfected with *Usp8* (pCMV-HA-*Usp8*) or empty vector for 24 hours. The overexpression of *Usp8* in the transfected iBMDMs was confirmed by qRT-PCR analysis and immunoblotting (Fig. S1D; Fig. 1J). Next, the iBMDMs overexpressing *Usp8* were infected with *B. neotomae* for the invasion assay. The CFU analysis showed a significant reduction in the invasion of *B. neotomae* in *Usp8*-overexpressing macrophages compared to the cells transfected with the empty vector (Fig. 1K). Next, we wished to examine whether the effect of *Usp8* overexpression is regulated by inhibiting its function using the antagonist. The iBMDMs overexpressing *Usp8* were treated with DUB-IN-2 for 24 hours, followed by infection with *B. neotomae*/*B. neotomae*-GFP. We observed an enhanced intracellular load of *B. neotomae*/*B. neotomae*-GFP in *Usp8*-overexpressing cells that are treated with DUB-IN-2 as compared to cells treated with DMSO (Fig. 1L and M). The protein 14-3-3ζ is reported to bind to USP8, which negatively regulates the activity of USP8. Therefore, inhibition of USP8 and 14-3-3ζ interaction can lead to the constitute activation of USP8. We used the commercially available non-peptidic inhibitor of 14-3-3, BV02 that interferes with the interaction of USP8 with 14-3-3ζ, followed by *Brucella* infection studies (32, 33). The iBMDMs were treated with BV02 or DMSO for 24 hours and infected with *B. neotomae* or *B. melitensis*. We confirmed that BV02 did not induce any cytotoxicity of iBMDMs upon treatment for 24 hours (Fig. S1E). In agreement with the overexpression studies, we observed a diminished invasion of *B. neotomae* or *B. melitensis* into iBMDMs treated with BV02 (Fig. 1; Panels N and O). Collectively, our experimental data show that *Usp8* negatively regulates the invasion of *Brucella* into macrophages.

## USP8 affects the invasion of *Brucella* into macrophages through the CXCR4 receptor

Since *Usp8* affected the invasion of *Brucella* into macrophages, we wished to examine whether *Usp8* regulates the membrane receptors required for *Brucella* entry. USP8 is known to negatively regulate the membrane localization and turnover of CXCR4, which is reported to be an essential receptor for the entry of *Brucella* into macrophages (12, 34). Since overexpression of *Usp8* inhibited the invasion of *Brucella* into macrophages, we hypothesized that USP8 might exert this effect by depleting the membrane-localized CXCR4 through negative regulation of its turnover inside the cells by promoting proteasomal degradation. To examine this, we analyzed levels of plasma membrane-localized CXCR4 in iBMDMs transfected with HA-*Usp8* or empty vector. Twenty-four hours post-transfection, the cells were fixed and stained for HA-USP8 and endogenous CXCR4, followed by fluorescence microscopy analysis. We observed a decreased membrane-localized CXCR4 in the cells overexpressing *Usp8* compared to those transfected with the empty vector (Fig. 2A). Furthermore, to confirm whether USP8 can regulate the turnover of CXCR4, we examined the total and membrane-localized CXCR4 in iBMDMs treated with USP8 inhibitor, DUB-IN-2 or USP8 activator, BV02. The immunoblotting showed an enhanced level of CXCR4 in total cell lysates and the membrane fractions upon treatment with the USP8 inhibitor. In contrast, CXCR4 decreased in the cells treated with the USP8 activator, indicating the role of USP8 in regulating the turnover of CXCR4 (Fig. 2B through E). The overexpression of *Usp8* in iBMDMs also resulted in a diminished level of CXCR4 as compared to the empty vector (Fig. S2A). Furthermore, we examined the membrane

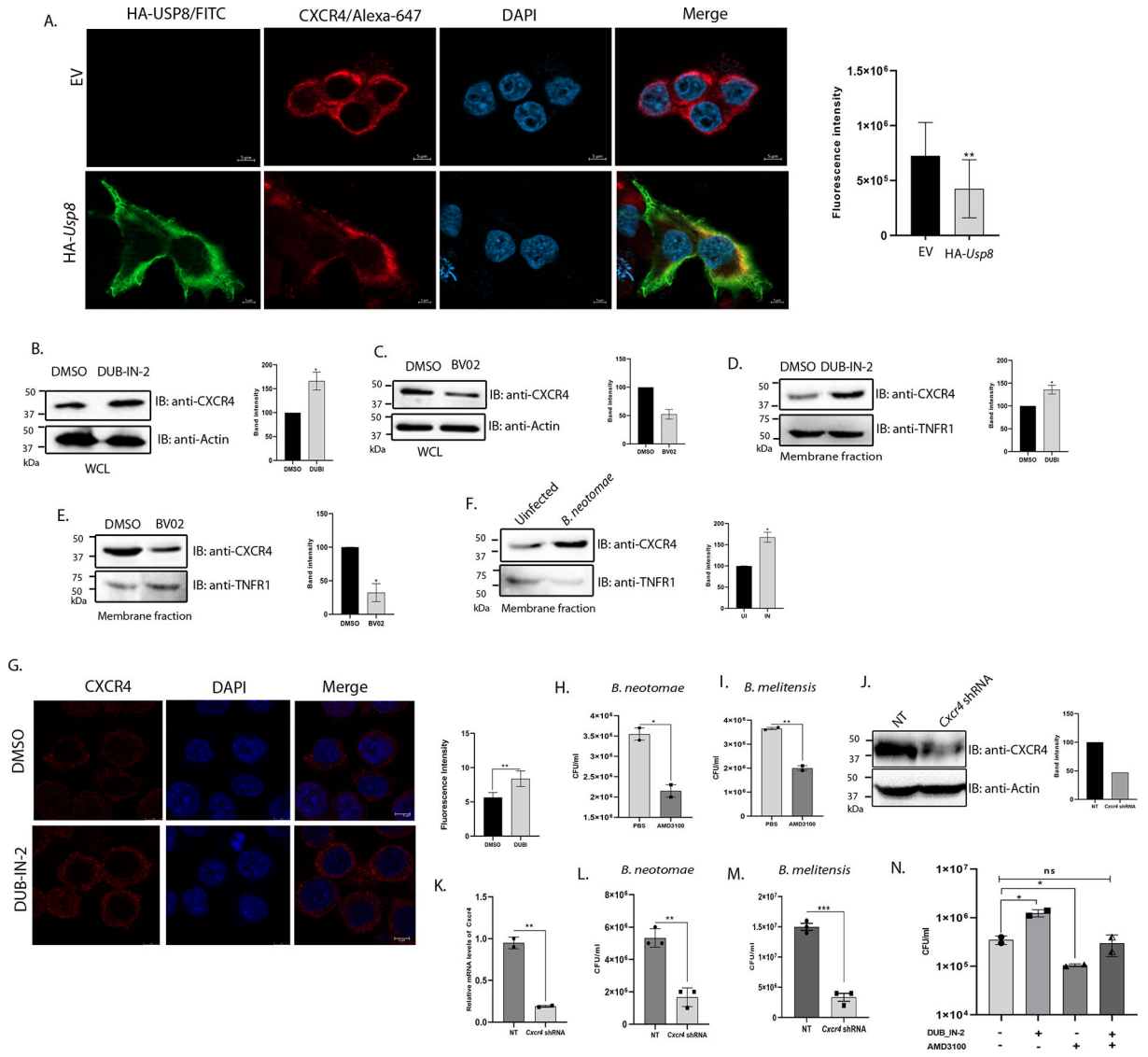


**FIG 2** USP8 affects the invasion of *Brucella* into macrophages through CXCR4. (A) Levels of CXCR4 on the plasma membrane of HEK293T cells overexpressing HA-*Usp8*. HEK293T cells were transfected with HA-*Usp8* or EV. Twenty-four hours post-transfection, the cells were stained with the anti-CXCR4 antibody, followed by Alexa Fluor 647-conjugated secondary antibody (red). HA-USP8 was stained with FITC-conjugated anti-HA antibody (green), and nuclei were stained with DAPI (blue). The cells were imaged using a laser confocal microscope at 63×. Scale bar, 5 µm. The image represents 12 different fields captured from cells transfected with either empty vector or HA-USP8. The right panel indicates the quantification of fluorescence intensity of CXCR4 using ImageJ software. (Panels B and C) Total levels of CXCR4 in iBMDMs treated with antagonists of USP8 or 14-3-3ζ. iBMDMs treated with DUB_IN-2 (B) or BV02 (C), or DMSO (vehicle) for 24 hours, followed by harvesting the cells and immunoblotting. To detect CXCR4, the membranes were probed with the anti-CXCR4 antibody, followed by HRP-conjugated anti-rabbit IgG. Actin was used as the loading control. The right panels indicate the densitometry of the CXCR4 band with respect to the actin band. (Panels D–F) Levels of plasma membrane-localized CXCR4 in iBMDMs treated with DUB-IN-2 (D) or BV02 (E) or infected with *B. neotomae* (F). The membrane fractions showing CXCR4 and TNFR1 isolated from the compound-treated or *Brucella*-infected cells, followed by immunoblotting. The right panel indicates the densitometry of the CXCR4 band with respect to the TNFR1 band. (G) iBMDMs showing membrane-localized CXCR4 upon treatment with DUB_IN-2 or DMSO. iBMDMs were treated with DUB_IN-2 or DMSO for 24 hours, followed by staining membrane-localized CXCR4 (red) as described earlier. Nuclei were stained with DAPI (blue). The cells were imaged using a laser confocal microscope at 63× magnification. Scale bar, 20 µm. The image represents 12 different fields captured from cells treated with either DMSO or DUB-IN-2. Right panel indicates the quantification of fluorescence intensity of CXCR4 using ImageJ software. (Panels H and I) *Brucella* invasion assay showing the CFU count of *B. neotomae* (H) or *B. melitensis* (I) in the presence of the CXCR4 inhibitor. (Panels J and K) The expression of *Cxcr4* in iBMDMs transfected with *Cxcr4*-specific or control shRNA construct. The cells were transfected with shRNA expression constructs for 48 hours, followed by analyzing the levels of *Cxcr4* by immunoblotting (J) and qRT-PCR (K). The right panel indicates the densitometry of the CXCR4 band with respect to the actin band. (Panels L and M) *Brucella* invasion assay in *Cxcr4*-silenced or control iBMDMs. The cells were transfected with *Cxcr4*-specific or non-targeting control shRNA.
(Continued on next page)

**FIG 2** (Continued)

Forty-eight hours post-transfection, the cells were infected with *B. neotomae* or *B. melitensis* for 30 min, followed by gentamicin treatment for 30 min to kill extracellular bacteria and quantification of invaded *B. neotomae* (L) or *B. melitensis* (M) by CFU enumeration. (N) *Brucella* invasion assay using iBMDMs treated with antagonists of USP8 and CXCR4, as indicated in the figure. iBMDMs were treated with DUB_IN-2 or AMD3100 or both DUB_IN-2 and AMD3100 for 24 hours, followed by infection with *B. neotomae* and enumeration of CFU. A representative result from at least two biological replicates is shown. The data are presented as the mean ± SD (*$P < 0.05$; **$P < 0.01$; ***$P < 0.001$, ns > 0.05). WCL, whole-cell lysate; EV, empty vector; ns, non-significant.

localization of CXCR4 in the *Brucella*-infected macrophages. The iBMDMs were infected with *B. neotomae* for 4 hours, followed by isolation of plasma membrane fraction and immunoblotting. An enhanced membrane-localized CXCR4 was detected in iBMDMs infected with *B. neotomae* compared to the uninfected cells (Fig. 2F). Our fluorescent microscopy studies also showed an enhanced level of CXCR4 on the plasma membrane in iBMDMs that are treated with USP8 inhibitor or infected with *B. neotomae* as compared to the controls (Fig. 2G; Fig. S2B).

Subsequently, we analyzed the role of *Cxcr4* on the invasion of *Brucella* into the macrophages. iBMDMs were treated with the antagonist of CXCR4, AMD3100, or vehicle control for 24 hours, followed by analyzing the invasion of *B. neotomae* or *B. melitensis*. We observed a significant decline in the entry of *Brucella* into the cells that are treated with AMD3100 as compared to the vehicle-treated cells (Fig. 2H and I). To confirm the experimental data further, we silenced *Cxcr4* expression in iBMDMs using shRNA. The iBMDMs transfected with *Cxcr4*-specific shRNA construct showed decreased level of *Cxcr4* expression as demonstrated by qPCR and immunoblotting (Fig. 2J and K). We observed a diminished invasion of *B. neotomae* or *B. melitensis* in *Cxcr4*-silenced iBMDMs compared to the cells transfected with the control shRNA (Fig. 2L and M). The experimental data suggest that the CXCR4 receptor plays an essential role in the entry of *Brucella* into the macrophages.

Furthermore, to link the role of USP8 and CXCR4 in *Brucella* invasion, we examined the combined effect of USP8 and CXCR4 antagonists upon entry of *Brucella* into macrophages. The iBMDMs were treated with DUB-IN-2 or AMD3100 or both the antagonists, followed by invasion assay. As anticipated, the higher *Brucella* invasion observed in macrophages treated with USP8 inhibitor was regulated by treatment with CXCR4 inhibitor (Fig. 2N). Our experimental data suggest that CXCR4 acts as an active receptor for *Brucella* invasion, and USP8 negatively regulates the plasma membrane localization of CXCR4, which interferes with the invasion of *Brucella* into macrophages.

## *Brucella* modulates the expression of *Usp8* in macrophages

Since *Usp8* negatively regulated the invasion of *Brucella* into macrophages, we speculated that *Brucella* might modulate the expression of *Usp8* to overcome its impact on infecting the macrophages. Therefore, we examined the endogenous levels of *Usp8* in the macrophages infected with *B. neotomae* or *B. melitensis* at various time points post-infection. We observed a significant suppression of mRNA expression of *Usp8* at the early time points up to 4 hours and restoration of *Usp8* levels by 8 hours in the macrophages infected with *B. neotomae* or *B. melitensis* (Fig. 3A and B). To confirm the experimental data, we examined the endogenous level of USP8 protein by immunoblotting in the *B. neotomae*-infected macrophages. In agreement with the mRNA expression data, the protein level of USP8 was also decreased at the early time points, and the expression was restored by 8 hours post-infection (Fig. 3C). Next, we sought to examine whether *Brucella* actively modulates the expression of *Usp8* in the infected macrophages. To examine this, iBMDMs were infected with heat-killed *B. neotomae*, followed by analyzing the *Usp8* expression level by qRT-PCR and immunoblotting. Interestingly, heat-killed *B. neotomae* did not modulate the expression of *Usp8*, indicating the requirement of live *Brucella* for suppressing the expression of *Usp8* (Fig. 3D and E).

Our experimental data suggest that *Brucella* modulates *Usp8* at the transcriptional level, as mRNA expression levels of *Usp8* were also affected. Various signaling processes

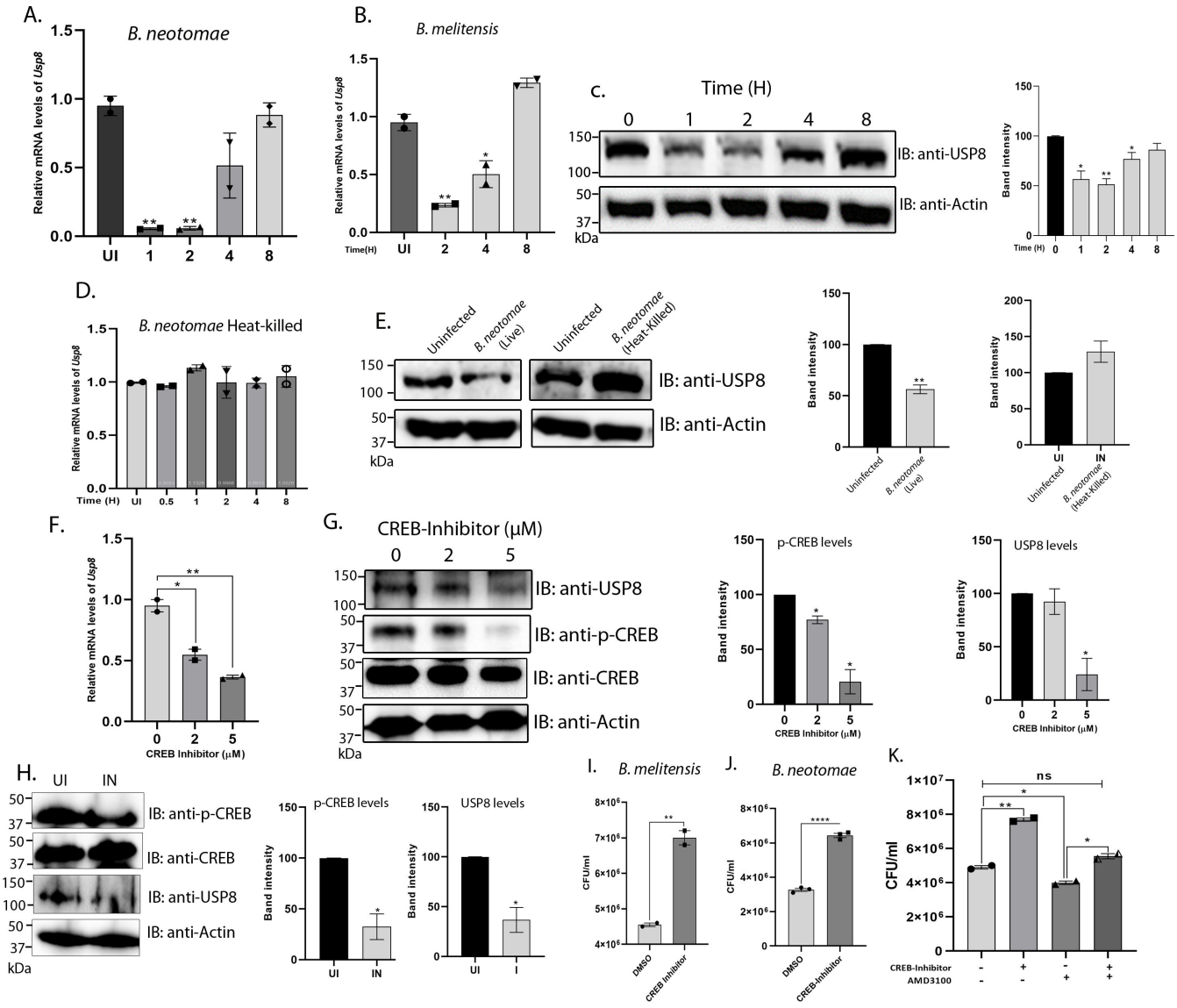


**FIG 3** *Brucella* modulates the expression of *Usp8* in macrophages. (Panels A and B) Endogenous levels of *Usp8* in iBMDMs infected with *Brucella*. iBMDMs were infected with *B. neotomae* (A) or *B. melitensis* (B), and *Usp8* levels were quantified at indicated time points by qRT-PCR. The expression of *Usp8* was normalized with the internal control, *Gapdh*, and the relative mRNA expression was determined compared to the uninfected cells. (C) Immunoblot showing USP8 levels in the *B. neotomae*-infected iBMDMs. The cells were infected with *B. neotomae* for the indicated time points, followed by cell lysis and immunoblotting. The right panel indicates the densitometry analysis of USP8 bands normalized with the actin bands. (D) The endogenous level of *Usp8* in the iBMDMs infected with heat-killed *B. neotomae*. The cells were infected with heat-killed *B. neotomae* for the indicated time points, followed by quantification of *Usp8* level by qRT-PCR. (E) Immunoblot showing USP8 levels in iBMDMs infected with live or heat-killed *B. neotomae*. The cells were subjected to immunoblotting 4 hours post-infection, followed by detection of endogenous levels of USP8. The right panel indicates the densitometry analysis of USP8 bands normalized with the actin bands. (Panels F and G) The endogenous levels of *Usp8* in iBMDMs treated with CREB inhibitor. The cells were treated with indicated concentrations of CREB inhibitor for 3 hours, followed by quantification of mRNA expression of *Usp8* by qRT-PCR analysis (F) or immunoblotting to detect the protein levels of USP8 and phosphorylated CREB (G). The right panel indicates the densitometry analysis of USP8 and p-CREB bands normalized with actin bands. (H) Immunoblot showing USP8 and p-CREB in iBMDMs-infected *B. neotomae*. The cells were infected for 4 hours, followed by cell lysis and immunoblotting to detect the endogenous levels of USP8 and phospho-CREB. The right panel indicates the densitometry analysis of USP8 and p-CREB bands normalized with actin bands. (Panels I and J) *Brucella* invasion assay in the presence of CREB inhibitor. iBMDMs were treated with CREB Inhibitor or DMSO (vehicle) for 3 hours, followed by infection with *B. neotomae* or *B. melitensis* for 30 min and quantification of invaded *B. neotomae* (I) or *B. melitensis* (J) by CFU enumeration. (K) *Brucella* invasion assay in iBMDMs treated with CREB and CXCR4 inhibitors. iBMDMs treated with AMD3100 (CXCR4 inhibitor) for 24 hours or CREB inhibitor for 3 hours as indicated, followed by infection with *B. neotomae* and enumeration of CFU for determining the intracellular bacteria. A representative result from at least two biological replicates is shown. The data are presented as the mean ± SD (**P* < 0.05; ***P* < 0.01; *****P* < 0.0001, ns > 0.05).

are reported to activate the transcription factor, Cyclic-AMP response element-binding protein (CREB) through its phosphorylation that, in turn, drives the expression of *Usp8* (35). Therefore, *Brucella* may affect the activation of CREB, which may downregulate the expression of *Usp8*. To examine this, we analyzed *Usp8* levels in macrophages treated with the antagonist of CREB. The iBMDMs were treated with increasing concentrations of CREB antagonist for 3 hours, followed by qRT-PCR analysis to examine *Usp8* mRNA level and immunoblotting to assess p-CREB and USP8 protein levels. We observed a dose-dependent depletion of the *Usp8* mRNA level as well as the protein levels of p-CREB and USP8 in the cells treated with the CREB antagonist (Fig. 3F and G). To examine whether *Brucella* infection affects the activation of CREB, the p-CREB and USP8 were evaluated in the infected and uninfected iBMDMs. We observed a significant suppression of CREB phosphorylation and USP8 expression in the *Brucella*-infected macrophages, demonstrating the role of *Brucella* in impacting *Usp8* transcription by inhibiting the activation of CREB (Fig. 3H).

Next, we analyzed whether CREB inhibitor interferes with the invasion of *Brucella* into macrophages. The iBMDMs were treated with the CREB inhibitor for 3 hours, followed by examining the invasion of *B. neotomae* or *B. melitensis*. We observed a significant enhancement of *B. neotomae* or *B. melitensis* invasion into the cells treated with CREB inhibitor compared to cells treated with the vehicle control, DMSO (Fig. 3I and J). Furthermore, we examined whether the effect of the CXCR4 inhibitor on *Brucella* invasion can be regulated by treating cells with the CREB inhibitor. To examine this, iBMDMs were first treated with the CXCR4 inhibitor for 24 hours, followed by treating the cells with the CREB inhibitor for 3 hours and *Brucella* invasion assay. As observed before, CXCR4 treatment resulted in a diminished invasion of *Brucella,* whereas this effect was counteracted by subsequent treatment of CXCR4-treated cells with the CREB inhibitor (Fig. 3K). Collectively, our experimental data suggest that CREB-mediated expression of *Usp8* affects the levels of CXCR4 that regulate the invasion of *Brucella* into macrophages.

## The *Brucella* effector protein, TcpB, downregulates the expression of *Usp8*

The TLR2/4 adaptor protein, TIRAP, is known to activate the CREB signaling pathway during the inflammatory response in microbial infections (36, 37). *Brucella* encodes the effector protein, TcpB, which is reported to promote the ubiquitination and degradation of TIRAP to attenuate the TLR2/4 signaling (20). Therefore, we sought to examine whether *TcpB* plays any role in the modulation of *Usp8* expression. To examine this, we transfected HEK293T cells with increasing concentrations of HA-*TcpB*, then analyzed the levels of *Usp8* by qRT-PCR and immunoblotting. Interestingly, *TcpB* suppressed the expression of *Usp8* in the transfected cells in a dose-dependent manner (Fig. 4A and B). To examine if other effector proteins of *Brucella* affect the *Usp8* expression, we tested two effector proteins, CpbB and BspI. HEK293T cells were transfected with increasing concentrations of mammalian expression plasmids harboring HA-*CbpB* and FLAG-*Bsp*I, followed by analyzing the levels of *Usp8*by qRT-PCR and immunoblotting (Fig. S3A through D). There was no suppression of *Usp8* with the overexpression of *CbpB* and *Bsp*I, indicating the specificity of *TcpB* in downregulating *Usp8* expression. To examine whether TcpB targets other host genes, we analyzed the mRNA levels of two host genes in the TLR2/4 signaling pathway, viz., *Myd88* and *Tirap* in the TcpB-overexpressing cells. We observed no change in the expression of *Myd88* and *Tirap* in the presence of TcpB (Fig. S3E and F). TcpB is a cell-permeable protein, and the recombinant TcpB protein is reported to get translocated into the macrophages (38). To further confirm the experimental data, recombinant TcpB protein was expressed infusion with MBP and purified. Next, iBMDMs were treated with purified MBP or MBP-TcpB proteins for 5 hours, then analyzed the level of USP8 expression by immunoblotting. We observed a significant suppression of USP8 in the cells treated with MBP-TcpB compared to MBP alone, confirming the role of TcpB in downregulating the *Usp8* expression (Fig. 4C). Next, we analyzed the levels of p-CREB and USP8 in the presence of TcpB. HEK293T cells were transfected with increasing concentrations of HA-*TcpB*, followed by analyzing

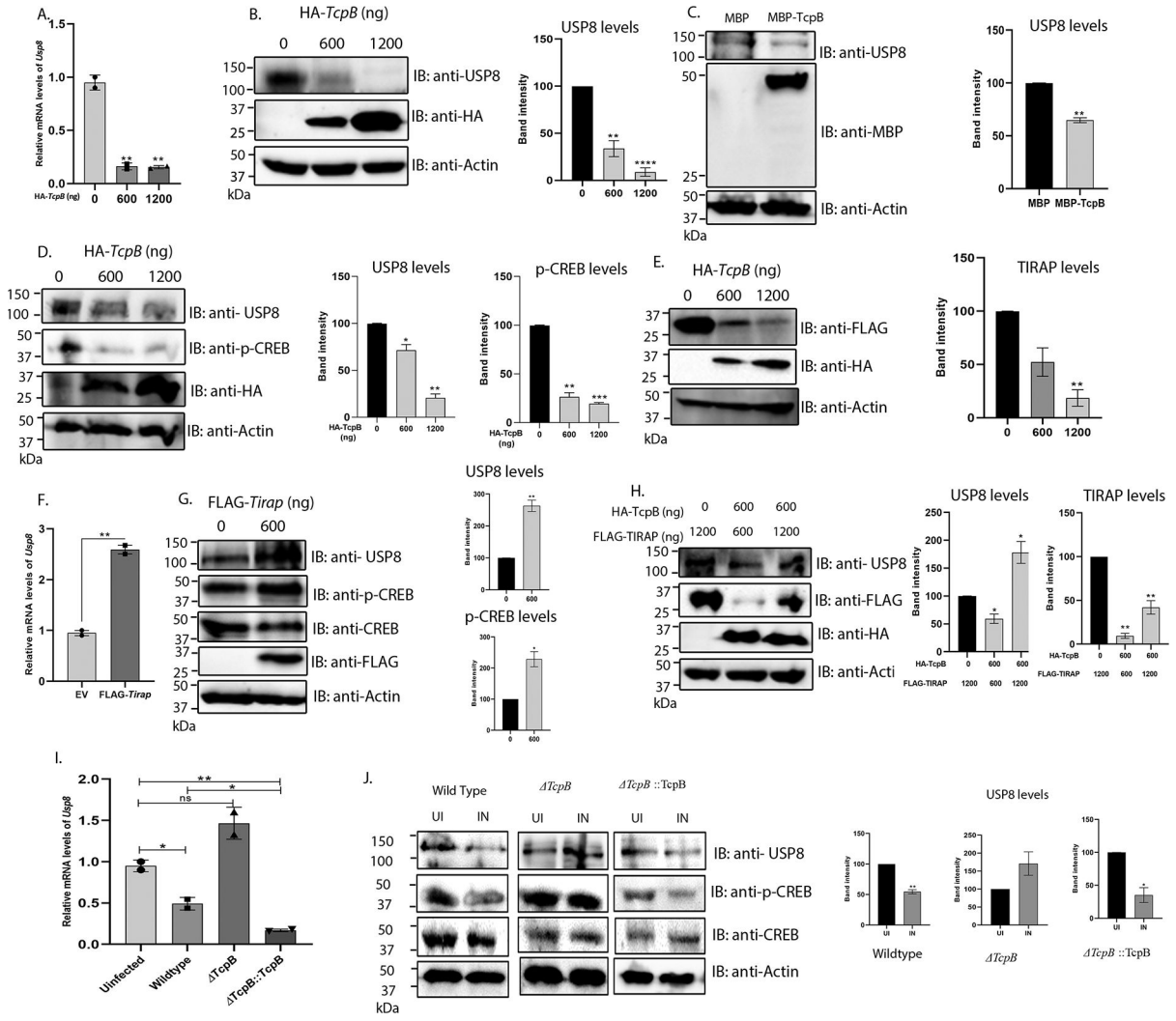


**FIG 4** The *Brucella* effector protein, TcpB, suppresses *Usp8* expression by targeting the TIRAP-CREB signaling pathway. (A) Endogenous levels of *Usp8* in iBMDMs overexpressing TcpB. The cells were transfected with the indicated concentrations of HA-TcpB or EV for 24 hours, followed by analyzing the mRNA expression level of *Usp8* by qRT-PCR. The *Usp8* expression data were normalized with *Gapdh*, and the relative mRNA expression of *Usp8* was determined with respect to the cells transfected with EV. (B) Immunoblot showing the levels of USP8 in the HEK293T cells overexpressing TcpB. The right panel indicates the densitometry analysis of USP8 bands normalized with actin bands. (C) Immunoblot showing the endogenous USP8 levels in iBMDMs treated with purified recombinant MBP-TcpB or MBP protein. The cells were treated with the purified proteins for 5 hours, followed by lysis and immunoblotting. HRP-conjugated anti-MBP antibody was used for detecting the MBP-TcpB or MBP alone. The right panel indicates the band intensity of USP8, which was normalized with actin bands. (D) Immunoblot showing the endogenous levels of USP8 and phospho-CREB in HEK293T cells transfected with increasing concentrations of HA-*TcpB*. The right panel indicates the densitometry analysis of USP8 and phospho-CREB bands normalized with actin bands. (E) Immunoblot showing the levels of FLAG-TIRAP in HEK293T cells co-transfected with indicated concentrations of HA-*TcpB* or EV for 24 hours. The membranes were probed with HRP-conjugated anti-FLAG and anti-HA antibodies to detect FLAG-TIRAP and HA-TcpB, respectively. The right panel indicates the band intensities of FLAG-TIRAP normalized with actin bands. (F) The mRNA expression level of *Usp8* in the iBMDMs transfected with FLAG-*Tirap*. Twenty-four hours post-transfection, cells were harvested and subjected to qRT-PCR analysis to quantify the levels of *Usp8*. (G) Immunoblot showing endogenous levels of USP8 and phospho-CREB in HEK293T cells transfected with indicated concentrations of FLAG-*Tirap* expression plasmid for 24 hours. The right panel indicates the densitometry analysis of USP8 and p-CREB bands normalized with the actin bands. (H) Immunoblot showing endogenous levels of USP8 in HEK293T cells transfected with indicated combinations of plasmids expressing FLAG-TIRAP and HA-TcpB. The right panel shows the densitometry analysis of USP8 and FLAG-TIRAP bands normalized with actin bands. (I) The mRNA expression levels of *Usp8* in iBMDMs infected with wild-type or *ΔTcpB B. neotomae* or *ΔTcpB*::TcpB *B. neotomae*. Four hours post-infection, the cells were harvested, followed by quantification of mRNA levels of *Usp8* by qRT-PCR. (J) Immunoblot showing the level of USP8 and p-CREB in iBMDMs infected with wild-type or *ΔTcpB B. neotomae* or *ΔTcpB*::TcpB *B. neotomae*. The cells were harvested 4 hours post-infection, followed by immunoblotting to detect endogenous USP8 and phospho-CREB. The right panel indicates the densitometry analysis of USP8 and phospho-CREB bands normalized with actin bands. A representative result from at least two biological replicates is shown. The data are presented as the mean ± SD (*$P < 0.05$; **$P < 0.01$; ***$P < 0.001$; ns > 0.05). EV, empty vector.

the endogenous levels of p-CREB and USP8 by immunoblotting. The experimental data showed a dose-dependent decrease in p-CREB and USP8 levels in the cells transfected with *TcpB*, confirming the role of TcpB in downregulating the *Usp8* through suppression of CREB phosphorylation (Fig. 4D).

To confirm that *TcpB* modulates *Usp8* gene expression through *Tirap*, we analyzed the levels of TIRAP and p-CREB in the *TcpB*-transfected cells. In concordance with the previous reports, we observed a dose-dependent degradation of TIRAP by TcpB in HEK293T cells co-transfected with HA-*TcpB*, or FLAG-*TIRAP* (Fig. 4E). Furthermore, a dose-dependent degradation of endogenous TIRAP was also observed in HEK293T cells transfected with the increasing concentrations of HA-TcpB (Fig. S3G). Next, we sought to examine whether TIRAP is required for the phosphorylation of CREB, which in turn promotes *Usp8* transcription. To analyze this, HEK293T cells were transfected with the plasmid-harboring FLAG-*Tirap* or empty vector, followed by evaluating the mRNA levels of *Usp8* by qRT-PCR and endogenous levels of p-CREB and USP8 by immunoblotting. As anticipated, we observed an enhanced *Usp8* transcription and enhanced endogenous p-CREB and USP8 levels in the cells that are overexpressing FLAG-*Tirap*, indicating the role of TIRAP in activating CREB and its downstream target, *Usp8* (Fig. 4F and G). To analyze whether overexpression of *Tirap* rescues *Usp8* suppression by TcpB, we performed a titration experiment where HEK293T cells were transfected with 600 ng of HA-*TcpB* and increasing concentrations of FLAG-*Tirap* (600 and 1,200 ng), followed by evaluating the expression of USP8. We observed a diminished suppression of USP8 by TcpB with the higher concentration of *Tirap,* indicating the effect of TcpB on *Usp8* is through *Tirap* (Fig. 4H). Collectively, our data show that degradation of TIRAP by TcpB prevents activation of CREB that impacts the transcription of *Usp8*.

To examine the role of TcpB in regulating the *Usp8* expression further, we generated *B. neotomae TcpB* knockout (Δ*TcpB*) mutant and its complemented strain with the wild-type *TcpB* (Δ*TcpB::TcpB*) and then confirmed by PCR analysis (Fig. S3H and I). Subsequently, the iBMDMs were infected with the *B. neotomae* wild-type Δ*TcpB* or *ΔTcpB::TcpB* strain and evaluated the expression of *Usp8* by qRT-PCR and protein levels of USP8 and phospho-CREB (p-CREB) by immunoblotting at 4 hours post-infection. We observed diminished expression of USP8 and p-CREB in the cells infected with the wild-type and *ΔTcpB:TcpB* complemented strains. In contrast, p-CREB and USP8 levels were unaffected in the iBMDMs infected with *ΔTcpB B. neotomae* (Fig. 4I and J). These experimental data indicate that *Brucella* modulates the expression of USP8 through its effector protein, TcpB. Next, we analyzed whether *TcpB* is pre-formed in the *Brucella* to affect the expression of USP8 at the early stages of its infection. To examine this, we analyzed the mRNA levels of *TcpB* in *B. neotomae* at lag, log, and stationary phases of bacterial cultures by qRT-PCR. We observed the expression of *TcpB* in the stationary phase of *Brucella* growth, indicating that TcpB is produced in the *Brucella* prior to infecting the host cells to modulate the *Usp8* expression (Fig. S3J).

## Inhibition of USP8 enhances the splenic load of *Brucella* in the infected mice

Our *in vitro* studies indicated that inhibition of USP8 resulted in an enhanced invasion of *Brucella* into macrophages through the plasma membrane receptor, CXCR4. Therefore, we wished to examine the effect of USP8 or CXCR4 antagonists *in vivo* using the mice model of brucellosis. Eight-week-old female BALB/c mice were infected with *B. melitensis*, followed by treatment with DUB_IN-2, BV02, AMD3100, or vehicle control for 3 days at 10 days post-infection. Subsequently, the mice were sacrificed, and the load of *B. melitensis* in the spleen was estimated by CFU analysis (Fig. 5A). The spleens from the mice treated with DUB_IN-2 showed a significantly higher number of *B. melitensis* than those treated with the vehicle control (Fig. 5B). In contrast, we observed a decreased number of *B. melitensis* in the spleen of mice that were treated with BV02 or AMD3100 as compared to the control mice (Fig. 5C and D). Furthermore, we observed diminished *Usp8* expression in the spleen of mice infected with *B. melitensis* compared to the uninfected mice (Fig. 5E). We have also analyzed the splenic load of *B. melitensis* in

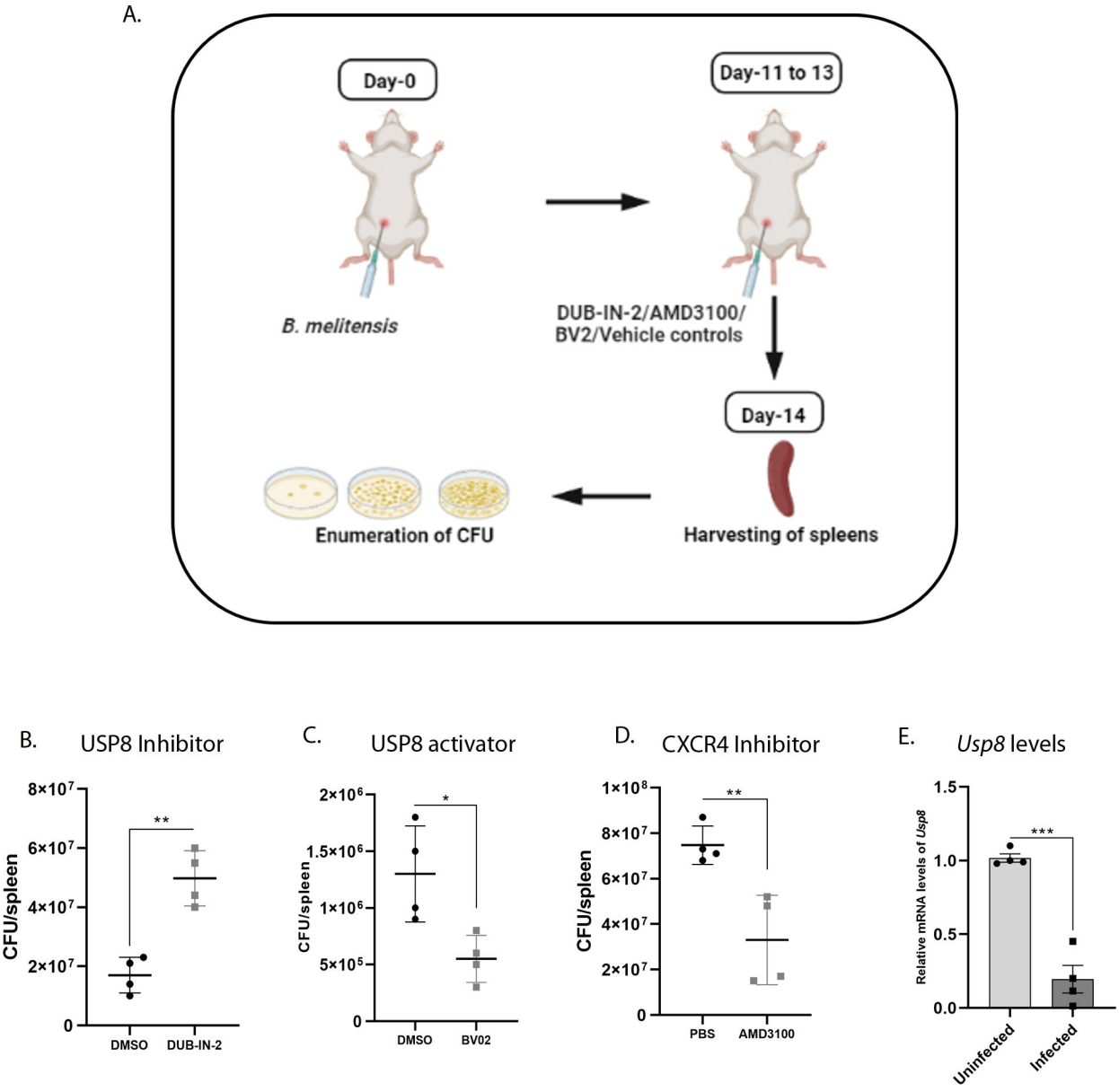


**FIG 5** USP8 plays a vital role in determining the load of *Brucella* in the infected mice. (A) Schematic showing the methodology used for examining the effect of inhibition of USP8/CXCR4 or activation of USP8 on the load of *B. melitensis* in the infected mice. (Panels B–D) Scatter plot showing the splenic load of *B. melitensis* in the mice treated with inhibitors of USP8/CXCR4 or activator of USP8. Eight-week-old female BALB/c mice were infected with *B. melitensis*. Ten-day post-infection, infected mice were treated with DUB_IN-2 (3 mg/kg) (B) or BV02 (3 mg/kg) (C) or AMD3100 (1 mg/kg) (D) or vehicle control for 3 days. Subsequently, the mice were sacrificed, and the load of *B. melitensis* in the spleen was estimated by CFU analysis. (E) The mRNA expression levels of *Usp8* in spleens infected with *B. melitensis*. Uninfected spleens were used as control. The data are presented as the mean ± SEM (**P* < 0.05; ***P* < 0.01; ****P* < 0.001).

mice that are treated with AMD3100, followed by infection. In agreement with the data obtained from macrophage infection studies, significant suppression of bacterial load was observed in the spleen of AMD3100-treated mice as compared to vehicle control (Fig. S4.A and B). Our *in vivo* experimental data suggest that the chemical inhibition of USP8 augments the load of *B. melitensis* in mice. In contrast, inhibition of CXCR4 or activation of USP8 leads to a remarkable reduction of *B. melitensis* survival in the infected mice.

## DISCUSSION

*Brucella* species successfully invade and multiply in the phagocytic cells by subverting various cellular processes (39). Their ability to prevent the intracellular killing and to create a safe replication permissive niche in the infected cells contributes to the chronicity of *Brucella* infection. *Brucella* also evades recognition or suppresses the activation of various host immune responses to chronically persist in the host (19, 40). However, minimal information is available on *Brucella* and host factors involved in host-pathogen interaction. Among many stages of the intracellular cycle of *Brucella*, gaining entry into the host cells is critical for initiating the infection cycle. Here, we identified the host protein, USP8, that plays an essential role in the invasion of *Brucella* into macrophages and in determining the bacterial load in the infected host.

Our studies unraveled a novel function of *Usp8*, where it plays a vital role in the host defense against *Brucella* infection. Downregulation of *Usp8* expression through siRNA or inhibiting its activity using chemical inhibitors potentiated *Brucella* invasion of macrophages and bacterial load in the infected mice, highlighting its role in the host defense. In contrast, enhancing the USP8 activity compromised the macrophage invasion and bacterial persistence in the infected mice, confirming USP8 as part of the host defense mechanism to avert pathogen entry and survival.

USP8 is reported to regulate the turnover and membrane localization of the plasma membrane-localized receptor, CXCR4. Though USP8 stabilizes various tyrosine kinase receptors such as EGFR and TβRII through its deubiquitylation property, it has a paradoxical function by enhancing the lysosomal degradation of CXCR4 (24, 41). CXCR4 is known to express on various immune cells, osteoclasts, and periodontal tissues. It has been reported to function as a co-receptor for the entry of HIV-1 virion into the host cells (42). The involvement of CXCR4 in the colonization of *Porphyromonas gingivalis* in periodontal tissues through binding to the fimbria has also been reported (43). The invasion of *Brucella* into macrophages involves the polymerization of actin filaments, receptor-mediated endocytosis, and interaction with various cytoskeletal regulators, such as small GTPases on the plasma membrane (11, 44). In addition, the CXCR4 receptor is reported to promote the entry of *Brucella* into the macrophages. Our studies revealed that USP8 affects the invasion of *Brucella* into macrophages through modulation of membrane localization and an overall turnover of the CXCR4 receptor. The inhibition of CXCR4 affected the invasion of *Brucella* into macrophages and its survival in the mice, underscoring the essential role of this receptor in invading the host cells. Furthermore, counteracting the effect of USP8 inhibition by blocking CXCR4 confirms the link between USP8 and CXCR4 in the invasion of *Brucella*. The data on mice infection studies also demonstrate the physiological relevance of USP8 suppression upon *Brucella* infection for persistence in the host and the role of membrane receptor, CXCR4, in the entry of *Brucella* into the host cells.

The depletion of CXCR4 through USP8 appears to be an efficient host defense strategy that operates by negatively regulating the receptors employed by pathogenic microorganisms to gain entry into the cells. However, the pathogens co-evolve with the host, which enables them to successfully overcome the defense mechanism to infect the host. In support of this view, we observed that *Brucella* downregulates the expression of *Usp8* at its early stages of infection to facilitate an unhindered invasion, which is crucial for its survival in the host. However, the normal expression of *Usp8* was restored after the invasion part of its life cycle, indicating the precise manipulation of host cellular processes according to the different stages of infection. In agreement with this observation, the upregulation of various scavenger receptors by *Brucella* through the host protein, FBXO22, has also been reported (45).

Intriguingly, we observed that only live *Brucella* could impart the suppression of *Usp8*, suggesting the role of a secreted effector protein to hijack the host signaling pathway involved in *Usp8* transcription. The changes in the expression levels of host genes upon *Brucella* infection are described in various instances previously, signifying the importance of host gene modulations for the *Brucella*-macrophage interaction (46).

## Graphical Summary

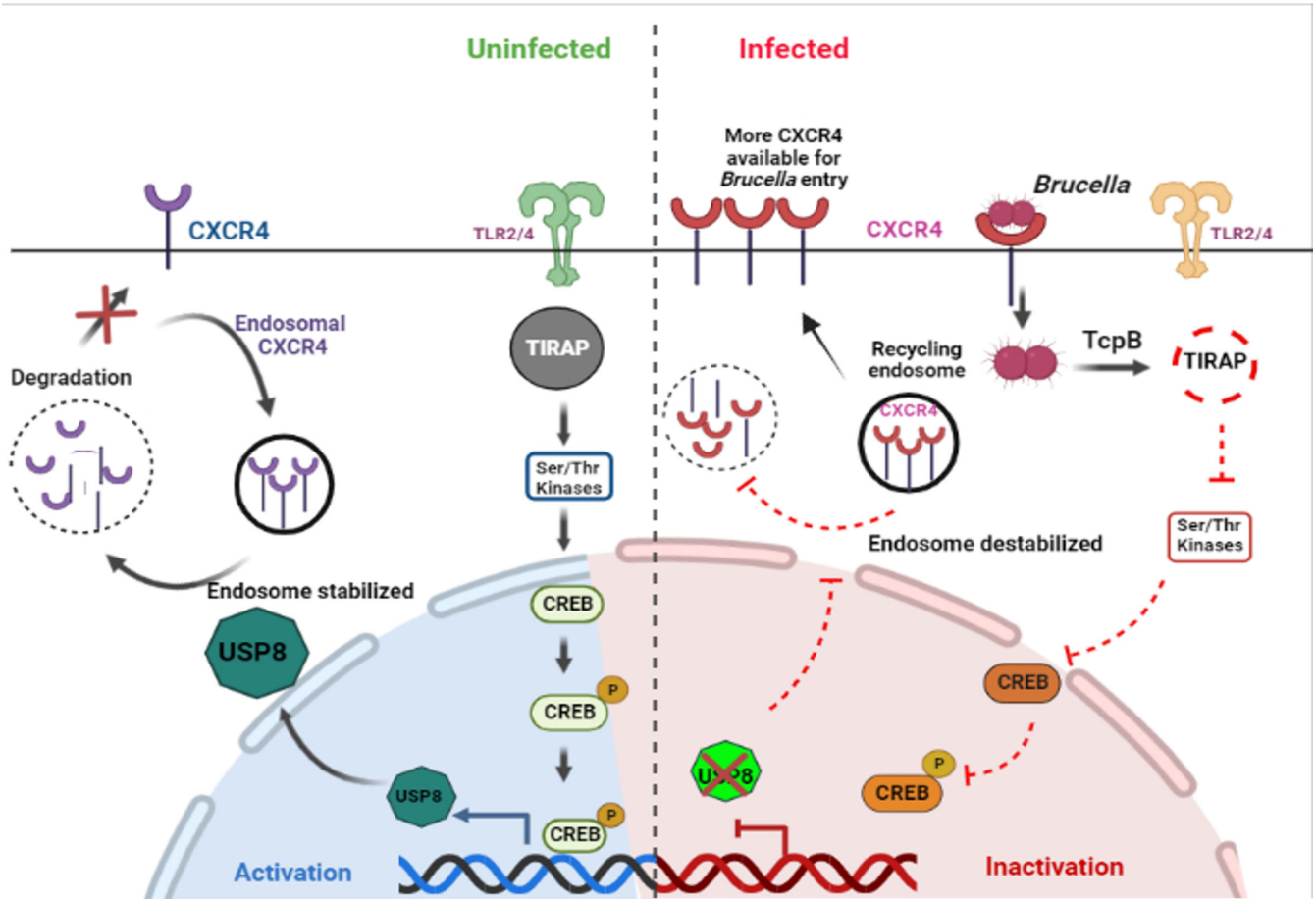


**FIG 6** Graphical summary depicting the role of *Usp8* in regulating the invasion of *Brucella* into the macrophages. Expression of *Usp8* through the TIRAP-CREB signaling pathway negatively regulates the turnover and plasma membrane localization of the CXCR4 receptor (left). Upon *Brucella* infection, the effector protein, TcpB, degrades TIRAP, preventing the CREB activation and transcription of *Usp8* (right). This promotes the recycling of endosomal CXCR4 and its availability on the plasma membrane, facilitating an enhanced *Brucella* invasion into macrophages.

Our subsequent experiments identified that the *Brucella* effector protein, TcpB, plays an essential role in negatively regulating *Usp8* expression through the TLR2/4 adaptor protein, TIRAP. CREB is a reported *Usp8* transcription factor that drives the expression of the *Usp8* gene (35). Since CREB acts as a key factor, which regulates downstream signaling events that are triggered during the microbial encounter to activate immune responses, we hypothesized that CREB might be an upstream target of *Brucella* to suppress *Usp8* gene transcription. Studies have shown that TIRAP-mediated signaling pathways can lead to the activation of CREB through its phosphorylation, resulting in the expression of various inflammatory and anti-inflammatory genes during microbial infections (37). This indicates that eliminating TIRAP through proteasomal degradation can compromise the CREB activation and expression of CREB-dependent genes. TcpB is known to induce ubiquitination and subsequent degradation of TIRAP to attenuate induction of pro-inflammatory cytokines to subvert the host innate immune responses (21). Our subsequent studies revealed that TcpB-induced TIRAP degradation prevents CREB activation and transcription of *Usp8*. Infection studies with Δ*TcpB B. neotomae* further confirmed the role of *TcpB* in *Brucella*-mediated suppression of *Usp8* through the CREB signaling pathway. The expression of *TcpB* in the stationary phase of *Brucella* culture suggests that TcpB is pre-formed in *Brucella* to facilitate downregulation of *Usp8*

at the time of invasion. Various studies have shown that *Brucella* employs its effector proteins to manipulate the host cellular pathways to create a replication permissive niche in the infected cells. The functional interaction of *Brucella* effectors, *BspB* and *RicA,* is reported to mediate Rab2-dependent transport in the intracellular life cycle of *Brucella* (15). Two recently identified *Brucella* effector proteins, *NyxA* and *NyxB,* are shown to modulate *SENP3* affecting the subcellular localization of nucleolar proteins (47).

In conclusion, our experimental data unravel a previously unknown role of *Usp8* as an essential player in the host defense against microbial infections. USP8 effectively prevents the invasion of *Brucella* into macrophages by depleting the membrane receptor CXCR4. Since *Brucella* species live in close association with the mammalian hosts, they have evolved efficient ways to invade the host cells. In support of this view, we found that *Brucella* negatively regulates the expression of *Usp8* at the early stages of the infection process using its effector protein, TcpB. TcpB exerts its effects through targeted degradation of TIRAP, thereby preventing the activation of CREB and attenuating the *Usp8* expression (Fig. 6). Our findings delineate the mechanisms the host employs to defend against microbial infection and the subversion of these innate defense strategies by the pathogen to establish the infection. Furthermore, the enhancement of the splenic load of *Brucella* upon USP8 inhibition and diminished *Brucella* survival upon activation of USP8 in mice underscores the role of USP8 in determining the host responses to the infection. This information can be extrapolated to other invasive infectious pathogens to understand their mode of infection and persistence in the host. In addition, various proteins and cellular pathways addressed in this study may serve as potential targets for developing novel therapeutics for brucellosis.

## ACKNOWLEDGMENTS

We thank the Department of Biotechnology, Ministry of Science and Technology, Government of India (Grant no. BT/PR12301/ADV/90/176/2014, BT/PR36546/ADV/90/284/2020, and BT/PR40896/AAQ/1/806/2020), for funding. K.J. acknowledges a Senior Research Fellowship from the Indian Council of Medical Research (71/2019-ECD-II, ICMR).

We thank the National Institute of Animal Biotechnology for providing the experimentation facility and the BSL3/A-BSL3 facility of UoH-NIAB for experiments with *B. melitensis*. We thank Shashikant Gawai and Rama Devi for helping with confocal and fluorescence microscopy.

G.K.R. conceived and designed the study. G.K.R. and K.J. prepared the manuscript, and V.M. and B.R.N. performed the experiments and analyzed the experimental data. All authors reviewed the results and approved the final version of the manuscript. Conceptualization, resources, supervision, and finding acquisition: G.K.R.; Methodology: G.K.R. and K.J.; Investigation: K.J., V.M., and B.R.N.; Writing–original draft: G.K.R. and K.J.; Writing–Review & Editing: G.K.R. and K.J.

## AUTHOR AFFILIATIONS

[1]Laboratory of Immunology and Microbial Pathogenesis, National Institute of Animal Biotechnology (NIAB), Hyderabad, Telangana, India
[2]Regional Centre for Biotechnology (RCB), Faridabad, India

## AUTHOR ORCIDs

Kiranmai Joshi http://orcid.org/0009-0009-0236-7643
Girish K. Radhakrishnan http://orcid.org/0000-0001-9088-0029

## FUNDING

| Funder | Grant(s) | Author(s) |
|---|---|---|
| Department of Biotechnology, Ministry of Science and Technology, India (DBT) | BT/PR12301/ADV/90/176/2014 | Girish K. Radhakrishnan |
| Department of Biotechnology, Ministry of Science and Technology, India (DBT) | BT/PR36546/ADV/90/284/2020 | Girish K. Radhakrishnan |
| Department of Biotechnology, Ministry of Science and Technology, India (DBT) | BT/PR40896/AAQ/1/806/2020 | Girish K. Radhakrishnan |
| Indian Council of Medical Research (ICMR) | 71/2019- ECD-II ICMR | Kiranmai Joshi |
| University Grants Commission (UGC) | 647/CSIR-UGG NET DEC.2018 | Binita Roy Nandi |

## AUTHOR CONTRIBUTIONS

Kiranmai Joshi, Formal analysis, Investigation, Methodology, Software, Validation, Visualization, Writing – original draft, Writing – review and editing | Varadendra Mazumdar, Data curation, Formal analysis, Investigation, Methodology, Software, Validation, Visualization | Binita Roy Nandi, Data curation, Investigation, Validation, Visualization | Girish K. Radhakrishnan, Conceptualization, Funding acquisition, Project administration, Resources, Supervision, Writing – review and editing

## ETHICS APPROVAL

All the experiments involving *B. melitensis* were conducted at the BLS3/Animal-BSL3 facility of UoH-NIAB on the campus of the University of Hyderabad, India. The experimental protocols were approved by the Institutional Biosafety Committee (Approval number: IBSC/Jul2020/NIAB/GR01) and Institutional Animal Ethics Committee (Approval number: IAEC/NIAB/2022/10/GKR) and BSL-3 Research Review Committee (Approval number: BSL3-Jan2022/002). Six- to eight-week-old female BALB/c mice were procured from the Small Animal Facility (SAF) of the National Institute of Animal Biotechnology (NIAB).

## ADDITIONAL FILES

The following material is available online.

### Supplemental Material

**Figure S1 (IAI00289-23-s0001.docx).** siRNA screening results.
**Figure S2 (IAI00289-23-s0002.docx).** Levels of CXCR4 in HEK293T cells and in uninfected or *B. neotomae*-GFP infected iBMDMs.
**Figure S3 (IAI00289-23-s0003.tif).** qPCR and immunoblot results.
**Figure S4 (IAI00289-23-s0004.docx).** Methodology and scatter plot.

## REFERENCES

1. Suárez-Esquivel M, Chaves-Olarte E, Moreno E, Guzmán-Verri C. 2020. *Brucella* genomics: macro and micro evolution. IJMS 21:7749. https://doi.org/10.3390/ijms21207749
2. Kurmanov B, Zincke D, Su W, Hadfield TL, Aikimbayev A, Karibayev T, Berdikulov M, Orynbayev M, Nikolich MP, Blackburn JK. 2022. Assays for identification and differentiation of *Brucella* species: a review. Microorganisms 10:1584. https://doi.org/10.3390/microorganisms10081584
3. Baldwin CL, Goenka R. 2006. Host immune responses to the intracellular bacteria *Brucella*: does the bacteria instruct the host to facilitate chronic infection Crit Rev Immunol 26:407–442. https://doi.org/10.1615/critrevimmunol.v26.i5.30
4. Franc KA, Krecek RC, Häsler BN, Arenas-Gamboa AM. 2018. Brucellosis remains a neglected disease in the developing world: a call for Interdisciplinary action. BMC Public Health 18:125. https://doi.org/10.1186/s12889-017-5016-y
5. Gheibi A, Khanahmad H, Kashfi K, Sarmadi M, Khorramizadeh MR. 2018. Development of new generation of vaccines for *Brucella abortus* Heliyon 4:e01079. https://doi.org/10.1016/j.heliyon.2018.e01079
6. Skalsky K, Yahav D, Bishara J, Pitlik S, Leibovici L, Paul M. 2008. Treatment of human brucellosis: systematic review and meta-analysis of randomised controlled trials. BMJ 336:701–704. https://doi.org/10.1136/bmj.39497.500903.25

7. Zai X, Yin Y, Guo F, Yang Q, Li R, Li Y, Zhang J, Xu J, Chen W. 2021. Screening of potential vaccine candidates against pathogenic *Brucella* spp. using compositive reverse vaccinology. Vet Res 52:75. https://doi.org/10.1186/s13567-021-00939-5
8. Salcedo SP, Chevrier N, Lacerda TLS, Ben Amara A, Gerart S, Gorvel VA, de Chastellier C, Blasco JM, Mege J-L, Gorvel J-P. 2013. Pathogenic brucellae replicate in human trophoblasts. J Infect Dis 207:1075–1083. https://doi.org/10.1093/infdis/jit007
9. Celli Jean, de Chastellier C, Franchini D-M, Pizarro-Cerda J, Moreno E, Gorvel J-P. 2003. Brucella evades macrophage killing via VirB-dependent sustained interactions with the endoplasmic reticulum. J Exp Med 198:545–556. https://doi.org/10.1084/jem.20030088
10. Celli J. 2019. The intracellular life cycle of *Brucella* spp. Microbiol Spectr 7. https://doi.org/10.1128/microbiolspec.BAI-0006-2019
11. Guzmán-Verri C, Chaves-Olarte E, von Eichel-Streiber C, López-Goñi I, Thelestam M, Arvidson S, Gorvel JP, Moreno E. 2001. GTPases of the Rho subfamily are required for *Brucella abortus* internalization in nonprofessional phagocytes: direct activation of Cdc42. J Biol Chem 276:44435–44443. https://doi.org/10.1074/jbc.M105606200
12. Reyes AWB, Arayan LT, Huy TXN, Vu SH, Kang CK, Min W, Lee HJ, Lee JH, Kim S. 2019. Chemokine receptor 4 (CXCR4) blockade enhances resistance to bacterial internalization in RAW264.7 cells and AMD3100, a CXCR4 antagonist, attenuates susceptibility to *Brucella abortus* 544 infection in a murine model. Vet Microbiol 237:108402. https://doi.org/10.1016/j.vetmic.2019.108402
13. Nakato G, Hase K, Suzuki M, Kimura M, Ato M, Hanazato M, Tobiume M, Horiuchi M, Atarashi R, Nishida N, Watarai M, Imaoka K, Ohno H. 2012. Cutting edge: *Brucella abortus* exploits a cellular prion protein on intestinal M cells as an invasive receptor. J Immunol 189:1540–1544. https://doi.org/10.4049/jimmunol.1103332
14. Celli J, Salcedo SP, Gorvel JP. 2005. *Brucella coopts* the small GTPase Sar1 for intracellular replication. Proc Natl Acad Sci U S A 102:1673–1678. https://doi.org/10.1073/pnas.0406873102
15. Smith EP, Cotto-Rosario A, Borghesan E, Held K, Miller CN, Celli J. 2020. Epistatic interplay between type IV secretion effectors engages the small GTPase Rab2 in the *Brucella* intracellular cycle. mBio 11:e03350-19. https://doi.org/10.1128/mBio.03350-19
16. Li C, Wang J, Sun W, Liu X, Wang J, Peng Q. 2022. The *Brucella* effector BspI suppresses inflammation via inhibition of IRE1 kinase activity during *Brucella* infection. J Immunol 209:488–497. https://doi.org/10.4049/jimmunol.2200001
17. Taguchi Y, Imaoka K, Kataoka M, Uda A, Nakatsu D, Horii-Okazaki S, Kunishige R, Kano F, Murata M. 2015. Yip1A, a novel host factor for the activation of the Ire1 pathway of the unfolded protein response during *Brucella* infection. PLoS Pathog. 11:e1004747. https://doi.org/10.1371/journal.ppat.1004747
18. Smith JA, Khan M, Magnani DD, Harms JS, Durward M, Radhakrishnan GK, Liu Y-P, Splitter GA. 2013. *Brucella* induces an unfolded protein response via TcpB that supports intracellular replication in macrophages. PLoS Pathog. 9:e1003785. https://doi.org/10.1371/journal.ppat.1003785
19. Jakka P, Namani S, Murugan S, Rai N, Radhakrishnan G. 2017. The *Brucella* effector protein TcpB induces degradation of inflammatory caspases and thereby subverts non-canonical inflammasome activation in macrophages. J Biol Chem 292:20613–20627. https://doi.org/10.1074/jbc.M117.815878
20. Alaidarous M, Ve T, Casey LW, Valkov E, Ericsson DJ, Ullah MO, Schembri MA, Mansell A, Sweet MJ, Kobe B. 2014. Mechanism of bacterial interference with TLR4 signaling by *Brucella* toll/interleukin-1 receptor domain-containing protein TcpB. J Biol Chem 289:654–668. https://doi.org/10.1074/jbc.M113.523274
21. Radhakrishnan GK, Yu Q, Harms JS, Splitter GA. 2009. *Brucella* TIR domain-containing protein mimics properties of the toll-like receptor adaptor protein TIRAP. J Biol Chem 284:9892–9898. https://doi.org/10.1074/jbc.M805458200
22. De Ceuninck L, Wauman J, Masschaele D, Peelman F, Tavernier J. 2013. Reciprocal cross-regulation between RNF41 and USP8 controls cytokine receptor sorting and processing. J Cell Sci 126:3770–3781. https://doi.org/10.1242/jcs.131250
23. Dufner A, Knobeloch KP. 2019. Ubiquitin-specific protease 8 (USP8/UBPy): a prototypic multidomain deubiquitinating enzyme with pleiotropic functions. Biochem Soc Trans 47:1867–1879. https://doi.org/10.1042/BST20190527
24. Berlin I, Schwartz H, Nash PD. 2010. Regulation of epidermal growth factor receptor ubiquitination and trafficking by the USP8·STAM complex. J Biol Chem 285:34909–34921. https://doi.org/10.1074/jbc.M109.016287
25. André ND, Silva VAO, Watanabe MAE, De Lucca FL. 2016. Knockdown of chemokine receptor CXCR4 gene by RNA interference: effects on the B16-F10 melanoma growth. Oncol Rep 35:2419–2424. https://doi.org/10.3892/or.2016.4620
26. Jakka P, Bhargavi B, Namani S, Murugan S, Splitter G, Radhakrishnan G. 2018. Cytoplasmic linker protein CLIP170 negatively regulates TLR4 signaling by targeting the TLR adaptor protein TIRAP. J Immunol 200:704–714. https://doi.org/10.4049/jimmunol.1601559
27. Yaseen I, Choudhury M, Sritharan M, Khosla S. 2018. Histone methyltransferase SUV39H1 participates in host defense by methylating mycobacterial histone-like protein HupB. EMBO J. 37:183–200. https://doi.org/10.15252/embj.201796918
28. De Clercq E. 2005. Potential clinical applications of the CXCR4 antagonist bicyclam AMD3100. Mini Rev Med Chem 5:805–824. https://doi.org/10.2174/1389557054867075
29. Li BX, Gardner R, Xue C, Qian DZ, Xie F, Thomas G, Kazmierczak SC, Habecker BA, Xiao X. 2016. Systemic inhibition of CREB is well-tolerated in vivo. Sci Rep 6:34513. https://doi.org/10.1038/srep34513
30. Kang YS, Brown DA, Kirby JE. 2019. *Brucella neotomae* recapitulates attributes of zoonotic human disease in a murine infection model. Infect Immun 87:e00255-18. https://doi.org/10.1128/IAI.00255-18
31. Kageyama K, Asari Y, Sugimoto Y, Niioka K, Daimon M. 2020. Ubiquitin-specific protease 8 inhibitor suppresses adrenocorticotropic hormone production and corticotroph tumor cell proliferation. Endocr J 67:177–184. https://doi.org/10.1507/endocrj.EJ19-0239
32. Gómez-Suárez M, Gutiérrez-Martínez IZ, Hernández-Trejo JA, Hernández-Ruiz M, Suárez-Pérez D, Candelario A, Kamekura R, Medina-Contreras O, Schnoor M, Ortiz-Navarrete V, Villegas-Sepúlveda N, Parkos C, Nusrat A, Nava P. 2016. 14-3-3 proteins regulate Akt Thr308 phosphorylation in intestinal epithelial cells. Cell Death Differ 23:1060–1072. https://doi.org/10.1038/cdd.2015.163
33. Mizuno E, Kitamura N, Komada M. 2007. 14-3-3-dependent inhibition of the deubiquitinating activity of UBPY and its cancellation in the M phase. Exp Cell Res 313:3624–3634. https://doi.org/10.1016/j.yexcr.2007.07.028
34. Berlin I, Higginbotham KM, Dise RS, Sierra MI, Nash PD. 2010. The deubiquitinating enzyme USP8 promotes trafficking and degradation of the chemokine receptor 4 at the sorting endosome. J Biol Chem 285:37895–37908. https://doi.org/10.1074/jbc.M110.129411
35. Bland T, Sahin GS, Zhu M, Dillon C, Impey S, Appleyard SM, Wayman GA. 2019. USP8 deubiquitinates the leptin receptor and is necessary for leptin-mediated synapse formation. Endocrinology 160:1982–1998. https://doi.org/10.1210/en.2019-00107
36. Mellett M, Atzei P, Jackson R, O'Neill LA, Moynagh PN. 2011. Mal mediates TLR-induced activation of CREB and expression of IL-10. J Immunol 186:4925–4935. https://doi.org/10.4049/jimmunol.1002739
37. Newton K, Dixit VM. 2012. Signaling in innate immunity and inflammation. Cold Spring Harb Perspect Biol 4:a006049. https://doi.org/10.1101/cshperspect.a006049
38. Radhakrishnan GK, Splitter GA. 2010. Biochemical and functional analysis of TIR domain containing protein from *Brucella melitensis*. Biochem Biophys Res Commun 397:59–63. https://doi.org/10.1016/j.bbrc.2010.05.056
39. Głowacka P, Żakowska D, Naylor K, Niemcewicz M, Bielawska-Drózd A. 2018. *Brucella* - virulence factors, pathogenesis and treatment. Pol J Microbiol 67:151–161. https://doi.org/10.21307/pjm-2018-029
40. Luo X, Zhang X, Wu X, Yang X, Han C, Wang Z, Du Q, Zhao X, Liu S-L, Tong D, Huang Y. 2017. *Brucella* downregulates tumor necrosis factor-α to promote intracellular survival *via* Omp25 regulation of different micrornas in porcine and murine macrophages. Front Immunol 8:2013. https://doi.org/10.3389/fimmu.2017.02013
41. Xie F, Zhou X, Li H, Su P, Liu S, Li R, Zou J, Wei X, Pan C, Zhang Z, Zheng M, Liu Z, Meng X, Ovaa H, Ten Dijke P, Zhou F, Zhang L. 2022. USP8 promotes cancer progression and extracellular vesicle-mediated CD8+ T

cell exhaustion by deubiquitinating the TGF-β receptor TβRII. EMBO J. 41:e108791. https://doi.org/10.15252/embj.2021108791
42. Xiao T, Cai Y, Chen B. 2021. HIV-1 entry and membrane fusion inhibitors. Viruses 13:735. https://doi.org/10.3390/v13050735
43. McIntosh ML, Hajishengallis G. 2012. Inhibition of porphyromonas gingivalis-induced periodontal bone loss by CXCR4 antagonist treatment. Mol Oral Microbiol 27:449–457. https://doi.org/10.1111/j.2041-1014.2012.00657.x
44. Watarai M, Kim S, Erdenebaatar J, Makino S, Horiuchi M, Shirahata T, Sakaguchi S, Katamine S. 2003. Cellular prion protein promotes *Brucella* infection into macrophages. J Exp Med 198:5–17. https://doi.org/10.1084/jem.20021980
45. Mazumdar V, Joshi K, Nandi BR, Namani S, Gupta VK, Radhakrishnan G. 2022. Host F-box protein 22 enhances the uptake of *Brucella* by macrophages and drives a sustained release of proinflammatory cytokines through degradation of the anti-inflammatory effector proteins of *Brucella*. Infect Immun 90:e0006022. https://doi.org/10.1128/iai.00060-22
46. von Bargen K, Gorvel J-P, Salcedo SP. 2012. Internal affairs: investigating the *Brucella* intracellular lifestyle . FEMS Microbiol Rev 36:533–562. https://doi.org/10.1111/j.1574-6976.2012.00334.x
47. Louche A, Blanco A, Lacerda TLS, Cancade-Veyre L, Lionnet C, Bergé C, Rolando M, Lembo F, Borg J-P, Buchrieser C, Nagahama M, Gérard FCA, Gorvel J-P, Gueguen-Chaignon V, Terradot L, Salcedo SP. 2023. *Brucella* effectors NyxA and NyxB target SENP3 to modulate the subcellular localisation of nucleolar proteins. Nat Commun 14:102. https://doi.org/10.1038/s41467-022-35763-8